

Author's responses to the second peer-review round. Here we present point-by-point replies to the referee's comments. The referee's comments are presented in plain text in this document, while our reply is indicated by italics.

The consequent changes made according to the referee's comments have improved the manuscript further. In this second revision of manuscript, deletions have been marked by ~~striketrough~~, whereas additional text are indicated by **red color**.

On behalf of my coauthors, yours sincerely,

Jonas Svensson

Anonymous Referee #1

The authors have addressed several of my main comments: they have added a relevant estimate of filter under catch, and satisfactorily addressed most minor comments.

Main comments “leftover”:

1) Carbonates. The authors have added clarification about the decomposition protocol they use, indicating that inspection of thermographs is sufficient to constrain artifacts of carbonates showing up as EC. However, I still recommend that assessments of uncertainty be improved/included.

a) Indeed, I had not understood the specific benefits of the EUSAAR_2 protocol previously; it certainly offers improved rejection of carbonates compared to IMPROVE. However, as pointed out before, Cavelli et al. 2010 deals with atmospheric aerosols that likely have much lower mineral dust loads than the samples here. Examination of their Figure 3 indicates a small response within the higher temperature times of their He/O₂ devolution from natural calcite. For mineral dust/EC ratios as in the snow, the question of potentially significant artifacts even with the EUSAAR_2 protocol still require assessment. Further the authors themselves suggest that ambiguous separation of EC/OC with their technique introduces scatter in their results; to quote from their response:

“The statement that the “good agreement” in fig.5 between the two optical measurements indicate that most of the scatter between TOM and PSAP is related to where the OCEC instrument determines to place the split point between OC and EC, still holds “

I do not understand how this could be reconciled with insensitivity to carbonates.

The “good agreement” statement actually refers to what is observed in Fig. 6, where we have a nice agreement, and not for fig. 5. We argue that in Fig. 5, where the data is quite scattered, the scatter is due to the difference in the optical and TOM techniques (and also in the previous revised manuscript we added the fact that it can also be related BC being mixed with SiC). We do not believe that this scatter has anything to do with carbonates. See further below, after comment section named b by the referee, on our extensive response on carbonates. In the revised manuscript we have decided to remove Fig. 6 from the paper due to comment #2 below, to notify that this is not further discussed.

b) Zhang et al. also provide extra information about this issue. On the one hand, since they use IMPROVE_A, their estimates likely significantly overestimate the artifacts using EUSAAR_2. However, citing their 20% estimate is likely not appropriate beyond their sample ensemble: their snow was significantly higher in EC content than that here (on average ~1500 ng/g, their Figure 4), and it is not known how the mineral content of their samples relates, in amount and composition to those here. I expect that carbonate artifacts scale only with carbonate concentration, not relative to EC load. Another way to present their results could be via examination of their figure 4, where 5 samples were acidified to test carbonate contamination, and on average, shifted downwards in EC content by approximately 200ng/g each.

We certainly agree with the reviewer that the presence of carbonates in atmospheric and snow samples collected from different areas of the world is a complicated issue. Also we agree that it's not necessary advisable to compare the uncertainties of carbonates to atmospheric samples to our snow samples. Thus,

we present clarifications to our previous review responses and revisions both here and in the revised manuscript.

According to tests made on the EUSAAR_2 protocol carbonate carbon (CC) evolves in the fourth stage of the organic carbon analysis step at ca. 650°C (Cavalli et al., 2010; Karanasiou et al., 2011). Karanasiou et al. (2011) tested the quantification of carbonate carbon (CC) during thermal-optical measurements by preparing test samples of “precipitated CaCO₃ suspended in a clean chamber and sampled on a quartz fibre filter as aerosol particles”, and analyzing these with the EUSAAR_2 protocol. Their tests confirm that at lower CC concentrations all CC evolve in the inert organic carbon (OC) quantification stage in the EUSAAR_2 protocol (Karanasiou et al., 2011, Fig. 4), and even at the highest tested amount of 56 µg CC on the filters, which corresponds to extreme desert dust events in southern Europe, 95 % of the CC was detected in the OC analysis step of EUSAAR_2 (Karanasiou et al., 2011, Fig. 5). The CC evolved in the OC analysis phase does not interfere with elemental carbon (EC) measurements. The studied CC concentration range in Karanasiou et al. (2011) covered extreme dust events reported in literature (CaCO₃ representing 40 % of the PM₁₀ aerosol particle number), and it can be expected that such concentrations cover at least a majority of our snow samples, also from the Himalaya, although the tested samples were aerosol samples and ours are from snow.

Consequently, visual inspection of the thermograms during the EUSAAR_2 protocol evidently informs us about the CC load on the filters. As mentioned in the previous review response round, none of our samples showed a large peak in the 650 °C stage of the OC measurement. Thus, our samples show similar peaks in the fourth OC analysis step as in Karanasiou et al. (2011) in Figure 4, which indicates low CC concentrations and subsequently all CC evolving in the OC quantification stage. Consequently, there is no reason to suspect any meaningful interference of CC with our EC measurements. Furthermore, also some of OC still evolves in the fourth OC temperature step at the same time with CC, and thus big peaks in this step would not automatically indicate high CC concentrations. Due to this, it is also often not possible to directly infer CC concentrations from these thermal-optical measurements.

While acidification of the filters with HCl is suggested for the IMPROVE protocol to remove CC before OC/EC quantification, this step is not necessary or even recommendable for the EUSAAR_2 protocol. Indeed, acid fumigation has shown to cause irreversible damage for common OC/EC analyzers due to possible incomplete volatilization of the residual acid (Jankowski et al., 2008) and is therefore generally not recommendable. Furthermore, fumigation has been shown to cause intense charring phenomena in ambient aerosol samples which may lead to severe overestimation of EC in the samples (Jankowski et al., 2008). This is demonstrated also by aerosol samples collected from the northern slope of the Himalayas at the Qomolangma Atmospheric and Environmental Observation and Research Station (Everest station) where 7 out of 20 acid fumigated samples recorded higher EC concentrations than non-acidified subsamples (Li et al. 2017), similar as in snow/glacier samples from the Tibetan Plateau where 1 out of 6 samples showed higher EC concentrations after acid fumigation (Zhang et al. 2017), in both cases using the IMPROVE_A protocol. Originally, the reviewer suggested that we would use the same methodology as for Himalayan glacier samples in Ming et al. (2008) to remove CC from our filters prior to analysis. In Ming et al. (2008) HCl was added directly onto the filters and subsequently rinsed away. Acidification is known to decrease BC particle size (Kaspari et al., 2011; Schwarz et al., 2013) and thus the approach of Ming et al. (2008) may lead to particle losses before EC analysis. Consequently, although acid fumigation effectively removes CC from the filters the above described cases show that acid treatments introduce other artifacts

to the EC quantification and increase the EC analysis uncertainties significantly. Thus, we don't see acidification as an appropriate approach to our samples, not even for testing.

In cases where there is reason to suspect high CC loading on the filters (e.g. based on big peaks in the fourth step of the OC analysis) Karanasiou et al. (2011) suggest direct determination of the CC content by acidification of the filters with phosphoric acid and determination of the CO₂ evolved. However, in case of our samples this step seems unnecessary as an indication of high CC loading is lacking. Importantly, mineral dust may be abundant on the Himalayan snow filters but based on our results it seems to consist mainly of other minerals than carbonates.

The reviewer is correct in stating that it is inappropriate to cite Zhang et al. (2017) for uncertainties by possible CC in our samples, as we have used different EC analysis protocols. Based on the information listed above, we have revised the respective part of the manuscript to clarify the uncertainties caused by possible CC loading on the filters.

2) On the strength/relevance of constraints on ambient observations of the laboratory test. I am concerned that the authors did not understand some portions my original major comment 2. To paraphrase: measurements of eBC (i.e. interpretation of light transmission through a complex and uncharacterized filter) with different instruments (PSAP and OC/EC instrument) were carried out. Comparison of these two determinations does not give information about the actual BC or eBC on the filter, but only on the precision and relationship of the light transmission measurement. This is why it is not a clear constraint on the evolved EC measurement, and provides no information about the validity of the separate thermally evolved EC measurement or the relationship to actual eBC. This is why my suggestion of analyzing the results in the context of relative loadings (known from known dilutions) might help: the scaling of results with particulate load for the two different techniques (light attenuation or thermal evolution) could reveal influences of minerals on the BC load determination.

If we understand the referee correctly, this applies to our figures 6 and 8 (and the discussion surrounding these two figures), where the optically derived BC is compared. The referee is correct in that we cannot use these optical BC estimates in this current manner in the paper. After further review we have decided to remove these two figures and the text section dealing with this in the revised manuscript. This can be done without undermining our main results and conclusions of the paper.

3) On the discussion of the trend of ratio with depth (Figure 13). I don't think adding the sentence "This observation is rather hypothetical, and it needs to be further explored." to this section sufficiently addresses my comment that there is no statistically relevant evidence for a trend.

While reviewing the manuscript, we decided to take out Fig. 13 and the discussion surrounding it. As correctly pointed out by the referee the statistics are not robust enough and more data is needed on this topic. Since discussion on the ratio between the optical and measured EC content with depth is not one of the main points of the paper we felt that removing Fig. 13 did not diminish the quality of the paper.

4) It is very unlikely that the R^2 value given for 5 is correct

As the reviewer correctly pointed out this R^2 value was incorrect. We rechecked the R^2 for all of the figures and updated the manuscript with correct numbers. It appears that this error crept in when the linear fit was forced through 0, but is now updated.

A separate question I am curious about is the potential impact of carbonate thermal decomposition in the OC stage of the EUSAAR_2 on the optical OC charring constraints; has this been considered?

No, this has not been considered and is not in the scope of this paper.

Anonymous Referee #2

The authors have addressed most of the comment satisfactorily, however there are several points that need further elaboration before I recommend publishing.

1. I repeat my original point below because there is no answer to the question why SiC is the best proxy for dust in two different regions that are subject to very different dust sources. I see the point that laboratory assays are important and they are valid, but the question is whether they are relevant. Why is SiC not a random choice?

p. 10, l. 16/22: Information on light absorbing constituents in SiC and stone crush are needed. The light absorption of mineral dust is strongly influenced by e.g., hematite, goethite etc. There is no point in determining a MAC of a “random” dust sample in the laboratory to apply it to the ambient samples with unknown contents of light absorbing constituents as the authors state themselves on p. 20, l. 13. It is not clear, why dust samples are tested in the laboratory that have no relevance for the ambient dust samples. Also, in Figure 7, the discrepancy between the gravimetrically determined SiC mass on filters and the estimated based on the MAC when values are $> 7 \text{ g / m}^2$ are just discarded without any further discussion. Is it possible, that the method does not work for high dust loadings? I suggest that the dust related aspects of the laboratory assays are drastically shortened to the information relevant for the ambient samples.

As noted above by the referee and to restate our standpoint, we think that the laboratory tests are important for this paper and they are relevant since they confirm that our laboratory technique is suitable for analysis of ambient samples. In a sense SiC was a randomly chosen test material, but it appeared to be the most relevant for our laboratory study since it has a grey-white-blueish color, compared to the completely black color of the laboratory soot. Optically we obtained a MAC value for SiC that was roughly the same as for other reported mineral dust values. As noted in the manuscript, we made some tests on a different mineral sample for comparison. We consider that the approach to test some different mineral dust samples is sufficient since we did not have the possibility to test local mineral dust from the sampling areas.

2. Even though there is no data pointing towards local sources, this aspect needs to be discussed.

l. 13 – 27: What about local dust sources? There are most likely bare rock or mountain walls from which mineral dust can be deposited on the glacier. In general dust sources and in particular local dust sources can be highly variable so that any kind of interpretation in terms of trends is difficult, especially if no information about the origin is available. If the authors had mineral dust size distributions at least a statement on potential role of local sources if very large particles are present could be made.

Information on the mineral dust size distribution would have been very valuable information, as well as the chemical composition of the mineral, but it is not available with this data set. It is possible that the sources are local, along with long range transported dust. We believe that any sort of discussion on the sources for the dust is beyond the scope of this manuscript (since we do not have any data to support this kind of discussion).

3. My suggestion how to test the importance of LAI loading on the filter as described below has been ignored.

I. 28 – 34: The interpretation that the MAC is decreasing towards the top of the snow pit is not convincing and an explanation why this might be the case is missing completely. There are not enough data points to conclude a trend in the MAC. The profile rather shows that LAI deposition is highly variable. Towards the bottom of the snow pit the ratio is also lower and if the point at 10 cm depth were not as low as observed, probably no trend would be inferred. The authors introduced on p. 20 the hypothesis that potentially large loadings on filters play a role for the observed variability of the MAC (see comment further above). To test this and to develop a potential explanation why the MAC changes, I recommend plotting in Figure 13 the ratio of the optical and TOM EC versus the ratio of Dust/EC and OC/EC to check if there is a relation with the overall LAI content. Also, indicate in the figure which ratio is meant. In the conclusion, the potential reasons for the observation should be given as well.

This was an error on our part and we apologize for that. After further reviewing the manuscript and based on the comment from the other referee (please see comment 3 from referee 1) on this topic we have decided to delete Fig. 13 and the discussion surrounding it. Additional work and data is needed on this topic. As we have removed Fig. 13, there was no need to perform the referee's suggest test now either.

4. I do not agree with the authors' answer that there is no point in removing the outlier. While it is true that it shows the scatter in the data, and therefore it is important to include it in the figure, it also drives the correlation. It is located in a 'convenient' spot, because it moves the slope closer to 1. As the authors say if the outlier were not there the agreement would be poorer. This needs to be discussed.

Figure 8: Is the outlier at Sunderhunga taken into account for the linear regression? If so, what would the slope look like without? It would be even greater than 19 % and that is a relatively large deviation between the optical measurement of EC with TOM and the estimated EC based on the MAC and the PSAP data. What does this discrepancy mean for the validity of the methods?

We still feel that removing one single point should not be done, but rather as previously suggested, it should be done more systematically with data points above a certain limit (e.g. above $0.03 \text{ g m}^{-2} \text{ EC}$ content, which yields an identical slope). For the revised manuscript, however, we have deleted this text in light of comment #2 made by the other referee. Thus, there is no need for this to be further discussed.

Minor point, in my opinion the title should read: "Light-absorption of dust and elemental carbon in snow in the Indian Himalaya and the Finnish Arctic"

Agree, Thank you.

References

- Cavalli, F., Viana, M., Yttri, K.E., Genberg, J., and Putaud, J-P.: Toward a standardised thermal-optical protocol for measuring atmospheric organic and elemental carbon: the EUSAAR protocol, *Atmos. Meas. Tech.*, 3, 79–89, doi:10.5194/amt-3-79-2010, 2010.
- Jankowski, N., Schmidl, C., Marr, I.L., Bauer, H., and Puxbaum, H.: Comparison of methods for the quantification of carbonate carbon in atmospheric PM₁₀ aerosol samples, *Atmos. Environ.*, 42, 8055–8064, 2008.
- Karanasiou, A., Diapouli, E., Cavalli, F., Eleftheriadis, K., Viana, M., Alastuey, A., Querol, X., and Reche, C.: On the quantification of atmospheric carbonate carbon by thermal/optical analysis protocols, *Atmos. Meas. Tech.*, 4, 2409–2419, doi.org/10.5194/amt-4-2409-2011, 2011.
- Kaspari, S. D., Schwikowski, M., Gysel, M., Flanner, M. G., Kang, S., Hou, S., Mayewski, P. A.: Recent increase in black carbon concentrations from a Mt. Everest ice core spanning 1860–2000 AD. *Geophys. Res. Lett.*, 38, L04703, doi:10.1029/2010GL046096, 2011.
- Li, C., Yan, F., Kang, S., Chen, P., Han, X., Hu, Z., Zhang, G., Hong, Y., Gao, S., Qu, B., Zhu, Z., Li, J., Chen, B., and Sillanpää, M.: Re-evaluating black carbon in the Himalayas and the Tibetan Plateau: concentrations and deposition, *Atmos. Chem. Phys.*, 17, 11899–11912, doi.org/10.5194/acp-17-11899-2017, 2017.
- Ming, J., Cachier, H., Xiao, C., Qin, D., Kang, S., Hou, S., and Xu, J.: Black carbon record based on a shallow Himalayan ice core and its climatic implications, *Atmos. Chem. Phys.*, 8, 1343–1352, doi:10.5194/acp-8-1343-2008, 2008.
- Schwarz, J. P., Gao, R. S., Perring, A. E., Spackman, J. R., and Fahey, D. W.: Black carbon aerosol size in snow, *Sci. Rep.*, 3, 1356, doi:10.1038/srep01356, 2013.
- Zhang, Y., Kang, S., Li, C., Gao, T., Cong, Z., Sprenger, M., Liu, Y., Li, X., Guo, J., Sillanpää, M., Wang, K., Chen, J., Li, Y., Sun, S.: Characteristics of black carbon in snow from Laohugou No. 12 glacier on the northern Tibetan Plateau, *Sci. Tot. Environ.*, 607–608, 1237–1249, doi.org/10.1016/j.scitotenv.2017.07.100, 2017.

1 **Light-absorption of dust and elemental carbon in snow from in the Indian Himalaya**
2 **and the Finnish Arctic**

3

4 Jonas Svensson¹, Johan Ström², Niku Kivekäs¹, Nathaniel B. Dkhar^{3,4}, Shresth Tayal^{3,4}, Ved P.
5 Sharma^{3,4}, Arttu Jutila^{5*}, John Backman¹, Aki Virkkula¹, Meri Ruppel⁶, Antti Hyvärinen⁷, Anna Kontu⁸,
6 Henna-Reetta Hannula⁸, Matti Leppäranta⁵, Rakesh K. Hooda^{1,3}, Atte Korhola⁶, Eija Asmi¹, Heikki
7 Lihavainen¹

8 ¹Atmospheric Composition Research, Finnish Meteorological Institute, Helsinki, Finland

9 ²Department of Environmental Science and Analytical Chemistry, Stockholm University, Stockholm,
10 Sweden

11 ³The Energy and Resource Institute, New Delhi, India

12 ⁴The Energy and Resource Institute University, New Delhi, India

13 ⁵Institute for Atmospheric and Earth System Research, Faculty of Science, University of Helsinki,
14 Helsinki, Finland

15 ⁶Department of Environmental Sciences, University of Helsinki, Helsinki, Finland

16 ⁷Expert Services, Finnish Meteorological Institute, Helsinki, Finland

17 ⁸Arctic Research Center, Finnish Meteorological Institute, Sodankylä, Finland

18 *Now at Alfred Wegener Institute, Bremerhaven, Germany.

19

20 *Correspondence to J. Svensson (jonas.svensson@fmi.fi)*

1 **Abstract**

2 Light-absorbing impurities (LAI) deposited to snow have the potential to substantially affect the snow
3 radiation budget, with subsequent implications for snow melt. To more accurately quantify the snow
4 albedo, the contribution from different LAI needs to be assessed. Here we estimate the main LAI
5 components, elemental carbon (EC) (as a proxy for black carbon) and mineral dust in snow from the
6 Indian Himalaya and pared the results to snow samples from Arctic Finland. The impurities are
7 collected onto quartz filters and are analyzed thermal-optically for EC, as well as with an additional
8 optical measurement to estimate the light-absorption of dust separately on the filters. Laboratory tests
9 were conducted using substrates containing soot and mineral particles specially prepared to test the
10 experimental setup. Analyzed ambient snow samples show EC concentrations that are in the same range
11 as presented by previous research, for each respective region. In terms of the mass absorption cross
12 section (MAC) our ambient EC had surprisingly about half of the MAC value compared to our
13 laboratory standard EC (chimney soot), suggesting a less light absorptive EC in the snow, which has
14 consequences for the snow albedo reduction caused by EC. In the Himalayan samples, larger
15 contributions by dust (in the range of 50 % or greater for the light absorption caused by the LAI)
16 highlighted the importance of dust acting as a light absorber in the snow. Moreover, EC concentrations
17 in the Indian samples, acquired from a 120 cm deep snow pit (covering possibly the last five years of
18 snow fall), suggest an increase in both EC and dust deposition, ~~while at the same time proposing a~~
19 ~~tendency for a reduction in the MAC value with snow depth.~~ This work emphasizes the complexity in
20 determining the snow albedo, showing that LAI concentrations alone might not be sufficient, but
21 additional transient effects on the light-absorbing properties of the EC need to be considered and studied
22 in the snow. Equally imperative is to confirm the spatial and temporal representativeness of these data
23 by comparing data from several and deeper pits explored at the same time.

1 1. **Introduction**

2 The deposition of light-absorbing impurities (LAI) in snow influences the radiation budget and can
3 cause enhanced melting via snow darkening (Warren and Wiscombe, 1980). This process affects
4 regions with seasonal snow cover, leading to an earlier snow retreat, which has major implications for
5 thawing and biogeochemical processes acting in the ground (AMAP, 2011). In mountainous areas with
6 glaciers, the impurities perturb glacier properties and the hydrological cycle (e.g. Xu et al., 2009). The
7 impact on snow reflectance (albedo) from black carbon (BC) aerosol particles is of particular interest.
8 Being one of the most effective light-absorbing aerosols, BC enters the atmosphere by combustion of
9 carbon-based fuels, in activities including forest fires and anthropogenic burning of bio- and fossil fuels
10 (Bond et al., 2013). Because of its negative effect on snow albedo, considerable effort has been made
11 to globally quantify BC in snow (e.g. Doherty et al., 2010; Ming et al., 2008; Schmitt et al., 2015), as
12 well as in ice cores (e.g. McConnell et al., 2007; Ruppel et al., 2014; Xu et al., 2009).

13 The potential impact of LAI in snow and ice make the Himalaya a region of special interest. It contains
14 numerous glaciers which are in a general state of recession, although contrasting patterns have been
15 reported in different areas (e.g. Bolch et al., 2012; Kääb et al., 2012). Himalayan glaciers act as
16 freshwater sources for several major rivers in Asia, including Indus, Ganges, Brahmaputra, Mekong,
17 and Yangtze, thus having a vital part in millions of people's lives (e.g. Immerzeel et al., 2010). The
18 glaciers are especially susceptible to BC emissions, since India and China located in close proximity,
19 emit the most BC world-wide (Bond et al., 2013). A recent study by Ming et al. (2015) found a
20 decreasing trend in albedo during the period of 2000-2011 on Himalayan glaciers, and suggested rising
21 air temperatures and deposition of LAI to be responsible for the decrease. In light of the vast area of the
22 Himalayas, there is a lack of in-situ measurements of LAI on glaciers, which are crucial for modeling
23 work (Gertler et al., 2016). The lack of measurements is especially pronounced in the Indian Himalaya,
24 since previous measurements of LAI in Himalayan snow and ice have largely been confined to China
25 (e.g. Xu et al., 2006) and Nepal (e.g. Ginot et al., 2014; Kaspari et al., 2011; Kaspari et al., 2014; Ming
26 et al., 2008).

27 In addition to BC, other LAI can contribute significantly to the radiative balance of the cryosphere.
28 Recent research has identified mineral dust and microorganisms as having a more important role than
29 previously thought in the current decline in albedo of the Greenland Ice sheet and other parts of the
30 Arctic (e.g. Dumont et al. 2014, Lutz et al., 2016). Similarly, Kaspari et al. (2014) reported such high
31 dust concentrations in the snow of Himalayan Nepal that the contribution of dust in lowering the snow
32 albedo sometimes exceeded that of BC. The importance of dust has also been illustrated from other
33 regions, for example the Colorado Rockies, US, where dust causes a significantly earlier peak in runoff
34 (Painter et al. 2007). In the Arctic, Doherty et al. (2010) suggest that 30 to 50 % of sunlight absorbed
35 in the snowpack by impurities is due to non-BC constituents. Evidently, dust has an important role in

1 the cryospheric radiative balance. Differentiating between the different impurities in the snow is not
2 trivial, however, and requires more than one analytical technique (Doherty et al., 2016). Traditionally,
3 dust in snow has been quantified by gravimetrically measuring filters (e.g. Aoki et al., 2006; Painter et
4 al., 2012). Other methods consist of using transmitted light microscopy (Thevenon et al., 2009), a
5 microparticle counter to measure the insoluble dust (Ginot et al., 2014), or mass spectrometry (using
6 iron as a proxy for dust) (Kaspari et al., 2014).

7 At present, three primary methods are used to measure BC in snow and ice (see Qian et al., 2015, in
8 which they are extensively presented). Out of the three methods, two utilize filters to collect impurities
9 in a melted sample. The first filter method measures optically the spectrally resolved absorption by the
10 impurities using an integrating sphere integrating sandwich spectrophotometer (ISSW) (e.g. Doherty et
11 al., 2010; Grenfell et al., 2011). The second filter method is the thermal-optical analysis of filters (e.g.
12 Forsström et al., 2009; Hagler et al., 2007). The third, non-filter-based method, uses laser-induced
13 incandescence with a single particle soot photometer (SP2) (e.g. McConnell et al., 2007; Schwarz et al.,
14 2012).

15 Each measurement method has benefits and drawbacks. The SP2 is specific to refractory BC and is able
16 to provide estimates on the size of the BC particles. However, the SP2 has a size range limitation
17 (roughly 70–600 nm, depending on the instrument settings and nebulizer setup), which may result in
18 the underestimation of BC mass since particles in snow have been reported to be larger (Schwarz et al.,
19 2012; Schwarz et al., 2013). The use of filters, on the other hand, can provide a practical logistics
20 advantage for the collection of LAI in remote locations because it is difficult to maintain the necessary
21 frozen chain for the snow samples from the field to the laboratory for analysis. Particulate losses can be
22 very significant if a sample is not kept frozen, thus not providing accurate results. Filtering of liquid
23 samples can be conducted in the field, and the substrates are more easily stored and transported to the
24 laboratory. The ISSW method has the advantage that it measures light-absorbing constituents on the
25 filter indiscriminately. Thus, the ISSW method is not specific to BC, and requires interpretation of the
26 spectral response to determine the BC component. The thermal-optical method (TOM) provides an
27 actual measurement of elemental carbon (EC) that is instrumentally defined. EC is assumed to be the
28 dominant light-absorbing component of BC, and often EC and BC are used interchangeably in literature.
29 The sampling efficiency of quartz filters used in TOM is not well characterized for small particles (Lim
30 et al., 2014). However, smaller particles normally contribute little to total particulate mass (Hinds 1999).
31 Thus, each method for measuring BC in snow has both advantages and disadvantages.

32 Here we present observations of LAI in snow from two glaciers in the Sunderdhunga valley in the
33 Indian Himalaya, which have not to our knowledge, been explored previously with respect to LAI in
34 snow. Using a measuring approach whereby the TOM is combined with a custom-built particle soot
35 absorption photometer (PSAP), we perform laboratory tests to provide a correct interpretation of the

1 results. Our Himalayan observations are further compared to samples from Arctic Finland for their LAI
2 content.

3 **2. Methodology**

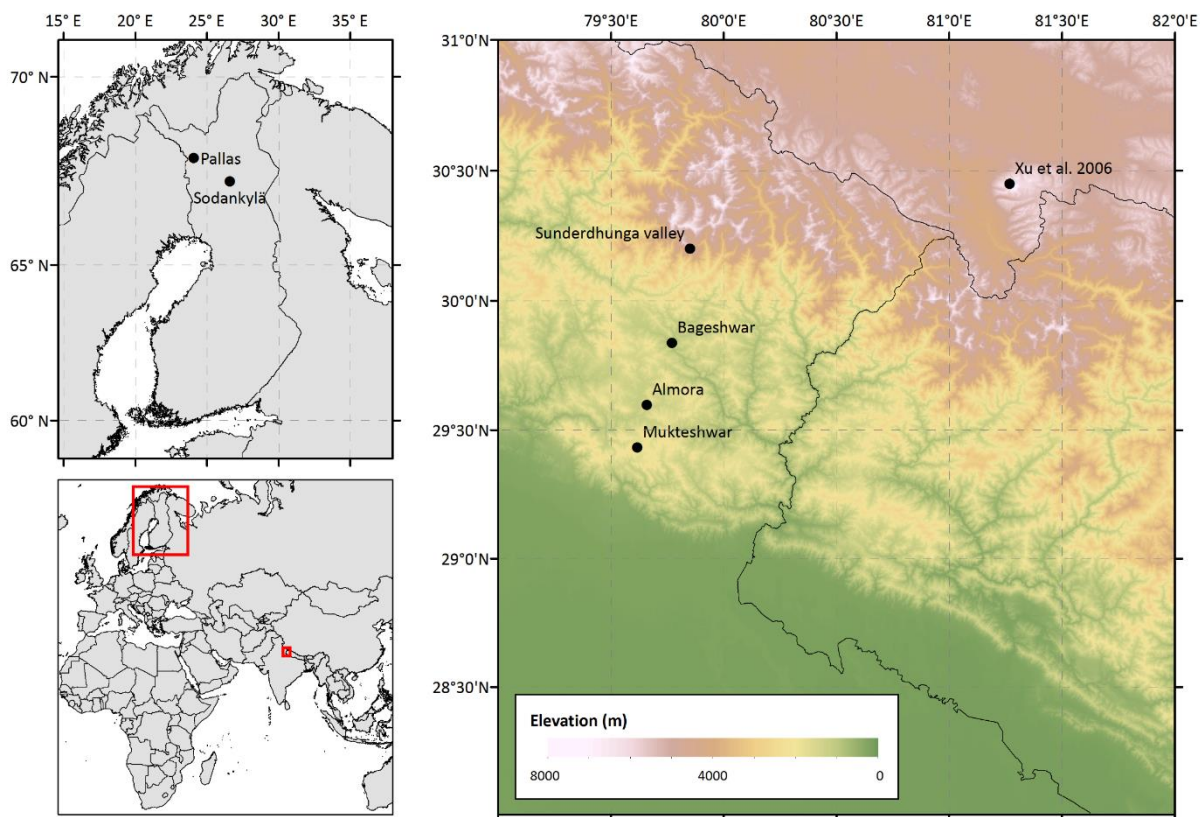
4 **2.1 Snow sample collection and site characteristics**

5 *2.1.1 The Indian Himalaya*

6 Snow samples were collected in September of 2015, during the Indian post-monsoon season, from two
7 adjacent glaciers in the Sunderdhunga valley (Figure 1). Bhanolti and Durga Kot glaciers (N 30° 12', E
8 79° 51') are located in the state of Uttarakhand, India. Facing northeast the glaciers cover an elevation
9 range of about 4400-5500 m a.s.l. and are two small valley-type glaciers in the Ganges hydrological
10 basin. Since the glaciers are situated at a relatively low altitude, they are more likely to be exposed to
11 BC than other Himalayan glaciers at a higher altitude, as BC has been shown to decrease with altitude
12 in other parts of the Himalaya (e.g. Kaspari et al., 2014; Ming et al., 2013; Yang et al., 2015). The
13 Sunderdhunga area does not have any major local pollution sources. Regionally, however, the small
14 towns of Bageshwar (~40 km S; population ~9000) and Almora (~70 km S; population ~34000), may
15 play a role. On a larger scale, the Sunderdhunga area is affected by the large-scale emissions from the
16 Indo-Gangetic Plain (IGP). Measurements of airborne BC and other aerosol particles at Mukteshwar, a
17 distance of ~90 km southwards at an altitude of 2200 m a.s.l., have shown a clear seasonal pattern in
18 atmospheric concentrations with emissions originating from the IGP (Hyvärinen et al., 2011;
19 Raatikainen et al., 2017). With a peak during the pre-monsoon season (March-onset of monsoon), the
20 BC loading has been reported to decrease by about 70 % at Mukteshwar during the monsoon (Hyvärinen
21 et al., 2011). Similarly, dust concentrations in the air have been shown to peak during the pre-monsoon
22 season at Mukteshwar (Hyvärinen et al., 2011). The pre-monsoon season, also known as the “dust-
23 season” in India, brings air masses from the Thar Desert transporting dust to the Himalaya (Gautam et
24 al., 2013). Dust from local sources has also been identified at Mukteshwar during this season
25 (Hyvärinen et al., 2011).

26 At Durga Kot glacier four snow pits with varying depths were dug at different elevations, while at
27 Bhanolti glacier one snow pit was dug (see table 1 for snow pits and sample details). Snow samples
28 were collected with a metal spatula in Nasco whirl-pak bags, and thereafter brought to base camp where
29 the snow was melted and filtered. Since it was not possible to maintain the crucial frozen chain for the
30 snow samples during transport back to the laboratory this approach of melting in the field was used for
31 the glacier snow samples. The snow was melted gently over a camping stove in enclosed glassware to
32 avoid contamination. The liquid samples were subsequently filtered through quartz fiber filters
33 (Munktell, 55 mm, grade T 293), in accordance to previous work (e.g. Forsström et al., 2009; Svensson

1 et al., 2013). Filters were dried in ambient conditions in petri dishes and thereafter transported to the
 2 laboratory for analysis (described in section 2.2).



3
 4 Figure 1. Map of sampling locations and sites discussed in text.

5 *2.1.2 Arctic Finland*

6 Snow samples collected in Finland originated from the seasonal snowpack of Sodankylä (N 67° 21' E
 7 26° 37') and Pallas (N 67° 58' E 24° 06') c.f. Figure 1. The Pallas samples were gathered in March and
 8 April of 2015 (n=10) from an open mire and in March of 2016 (n=2) from an area above the tree line
 9 (in close proximity of the Pallas Global Atmosphere Watch Station). More details of the Pallas sampling
 10 area are provided in Svensson et al. (2013) where EC in the snow was previously investigated. The
 11 sampled snow was confined to the top layers of the snowpack. The Sodankylä samples (n=15) are from
 12 the Finnish Meteorological Institute Arctic Research Center, where weekly surface snow samples (0-5
 13 cm) have been collected since 2009 (the first part of time series is presented in Meinander et al., 2013;
 14 where details of the area are provided). The samples used in this study originate from spring of 2013
 15 and 2014. The snow samples from Pallas and Sodankylä were collected in Nasco whirl-pak bags and
 16 stored in a frozen state until filtration. Samples were then melted in a microwave oven at each site's
 17 respective laboratory, and followed the same filtering procedure described above, according to e.g.
 18 Forsström et al. (2009) and Svensson et al. (2013).

1 **2.2 Light-absorbing impurities analysis**

2 To estimate the contribution to the reduction in transmission on the filter sample substrate due to
3 minerals, we compared the light transmission through the filter using the PSAP before and after heating
4 the sample as part of the TOM analysis. Since it is difficult to gravimetrically determine the dust content
5 on quartz filters, we decided to use this combined instrument approach to estimate the dust content. A
6 custom built PSAP (Krecl et al., 2007) was used for the optical measurements, and for the TOM a
7 Sunset Laboratory OCEC-analyzer was used to determine EC. A brief description of the OCEC-
8 analyzer and the PSAP is given below in sections 2.2.1 and 2.2.2, respectively.

9 The approach of measuring light transmission before and after heat treatment to estimate the different
10 light-absorbing components has been previously used for airborne sampled aerosol (e.g. Hansen et al.,
11 1993). In Hansen et al. (1993), filter samples were optically analyzed before and after being treated in
12 a 600°C furnace, in which the carbonaceous material was vaporized from the filter. These measurements
13 enabled them to obtain an estimate of the dust content on the filter. Lavanchy et al. (1999) followed a
14 similar optical and thermal approach to determine the BC and dust content of ice core samples. For the
15 EC measurement they used a two-step combustion procedure by Cachier et al. (1989), and in between
16 the thermal treatment they used a modified version of an aethalometer to measure the attenuation of
17 light through the filter. Our experimental method is analogous to that of Lavanchy et al. (1999).
18 However, as a Sunset Lab. OCEC-analyzer and a custom built PSAP were readily available to us, this
19 instrument configuration was used in our study. Because results from this type of analysis may be very
20 instrument specific, a series of laboratory tests (described in section 2.3) were conducted to confirm
21 reliability of the method before ambient snow samples were measured. The analysis procedure for the
22 filters (outlined further in section 2.3) was the same for the laboratory samples and the ambient samples.

23 *2.2.1 Elemental carbon analysis*

24 From a 10 cm² filter sample area, separate punches of 1 cm² were taken and analyzed for organic carbon
25 (OC) and EC content using a Sunset laboratory OCEC-analyzer (Birch and Cary, 1996) with the
26 EUSAAR_2 analysis protocol (Cavalli et al., 2010). First, in a helium atmosphere, the filter punch is
27 heated at different temperature steps. In this phase OC is volatilized and detected by a flame ionization
28 detector (FID). During the second stage, oxygen is introduced, and EC is released from the filter through
29 combustion. To account for pyrolysis (darkening of the filter) occurring during the first step, a laser (at
30 a 632 nm wavelength) measures the transmittance (or reflectance as an option for newer instruments)
31 continuously of the filter punch, and when the original value of the transmittance (measured before
32 thermal sequence starts) is attained during the second step separation between OC and EC is done. The
33 EC values reported here (referred to as EC_{TOM}) **were all corrected for pyrolysis accordingly.** ~~are based~~
34 ~~on the transmittance correction for pyrolysis since the PSAP operates also on the basis of transmittance~~
35 ~~through the substrate. An additional EC value provided by the OCEC-analyzer from the analysis is an~~

1 ~~optical EC (EC_{optical}), which is based on the monitored transmittance and absorption coefficients of the~~
2 ~~OCEC analyzer. Carbonates may be present in filter samples (Chow & Watson, 2002), and unless~~
3 ~~chemically removed before analysis, these particles will contribute to the OC fraction of the total~~
4 ~~particulate carbon content in the EUSAAR_2 protocol (Cavalli et al., 2010). For our samples,~~
5 ~~carbonates are assumed to be present in insignificant amounts since our visual inspection of the~~
6 ~~thermograms from analysis revealed no carbonate peak. Recent tests by Zhang et al. (2017), on acidified~~
7 ~~and non-acidified filter samples with snow from Tibet have showed less than 20 % discrepancy between~~
8 ~~treated and non-treated filter substrates.~~

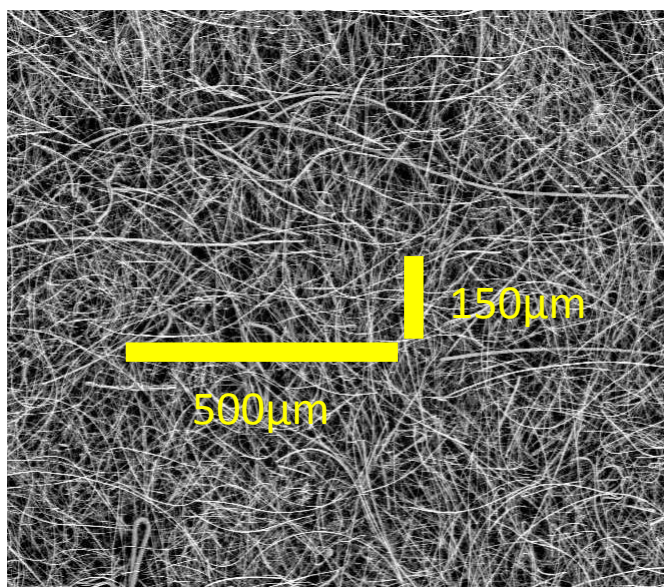
9 Uncertainties associated with the TOM method are mainly associated with uneven filter loading, loss
10 of particles to filtering containers, and the inefficiency of the filters to capture the impurities
11 (undercatch) (Forsström et al., 2013; Lim et al., 2014). For our filtering set-up the undercatch has been
12 estimated to ca. 22 % (Forsström et al., 2013), and is most likely significant for smaller sized particles,
13 since undercatch tests have indicated an inefficiency for smaller sized particles (Lim et al., 2014).
14 During OCEC-analysis, an artifact from samples with a high fraction of pyrolysis OC (Lim et al., 2014),
15 and the interference of an accurate split point determination from filters containing a high dust load can
16 also be considerable for the TOM method (Wang et al., 2012). **Generally, mineral dust may contain**
17 **carbonate carbon (CC) that may interfere with the OC and EC measurements unless it is chemically**
18 **removed prior to analysis. However, unlike in other OCEC analysis protocols (such as IMPROVE) here**
19 **chemical removal of CC was unnecessary, as in the EUSAAR_2 protocol CC evolves during the fourth**
20 **temperature step of the OC analysis (Cavalli et al., Karanasiou et al., 2011), and consequently CC does**
21 **not interfere with our EC quantification. In cases where CC is present in very high concentrations on**
22 **the filters, ca. 5 % of CC may evolve only during the EC analysis step causing potential overestimation**
23 **of EC (Karanasiou et al., 2011). As none of our filters indicated high CC concentrations during the**
24 **fourth temperature step of the OC analysis we assume only minor potential overestimation of our EC**
25 **results due to CC. Refraining from acid pretreatment of the samples is also advisable as incomplete**
26 **volatilization of residual acid is known to cause irreversible damage to the measurement instruments,**
27 **and furthermore the acid treatment has been shown to cause intense charring phenomena which may**
28 **lead to severe overestimation of EC (Jankowski et al., 2008).**

29 *2.2.2 Absorption measurements*

30 The PSAP uses a single diode at 526 nm as light source. The light is split by two light pipes which
31 illuminate two areas of 3.1 mm in diameter. The filter substrate is placed over these areas and individual
32 detectors below the filter measure the transmitted light. During normal operations, when measuring BC
33 in air, these two signals are used as sample and reference spots. The reference spot is exposed to particle
34 free air and the sample spot is exposed to particles present in the ambient air. In this experiment both
35 signals are used to measure the change in transmission by comparing the signal before and after the

1 filter has been analyzed using TOM. The signal change is related to the transmission from a particle
 2 free filter (filtered using Milli-Q (MQ) water and dried; the measurement procedure is further explain
 3 in 2.3).

4 The corrections required for the PSAP when used for air sampling is well documented (e.g. Bond et al.,
 5 1999; Virkkula et al., 2005), in particular this concerns enhanced absorption from the filter itself through
 6 multiple scattering effects from the filter fibers, and particle loading effects (shadowing and reduction
 7 in multiple scattering). However, these corrections are essentially uncharacterized for melted snow
 8 samples and the quartz fiber filters used. The fiber filters used are substantially thicker compared to
 9 what is normally used for PSAP measurements (Pallflex cellulose membrane filter) or the ISSW
 10 measurements (Nuclepore filter). Moreover, the filter substrate is very large in terms of surface area
 11 compared to the particles sampled. The geometry is very complex and in relation to a particle the
 12 substrate is more of a three dimensional web or sponge rather than a flat surface area on a filter. An
 13 example of a blank filter sample obtained by a scanning electron microscope is presented in Figure 2.
 14 The horizontal scale of 500 μm is for comparison, and the scale of 150 μm is to illustrate the relative
 15 thickness of the substrate.



16

17 Figure 2. Electron microscope image of a blank quartz fiber filter used in this study.

18 The basis for the optical attenuation measurements is the exponential attenuation of light as it passes
 19 through some medium, often described by the Bouguer-Lambert-Beer-law (Eq. 1).

20
$$I = I_0 e^{-\tau}, \quad (\text{Eq. 1})$$

21 where I_0 in our case is the light intensity through a clean filter and, I is the light intensity through a
 22 sample loaded filter. The exponent τ is the optical depth of LAI on the filter. For our study the multiple
 23 scattering absorption enhancement factor of the filter will be treated as a constant, but not given a

1 numerical value. Due to the geometry of the filter, corrections for any enhanced absorption due to co-
 2 existing scattering particles, and the loading effect, are not specifically considered. Hence, we will
 3 assume a linear relation between the logarithmic change in transmittance (T_r) of a filter and the optical
 4 depth (Eq. 2).

$$5 \quad \ln(T_r) = \tau_{TOT}, \text{ (Eq. 2)}$$

6 where $T_r = \frac{I_0}{I}$ and τ_{TOT} is the combined effect of all light absorbing impurities. Our interest was to
 7 estimate the relative contributions of EC (τ_{EC}) and mineral dust (τ_D) particles to measured optical depth
 8 according to equation 3.

$$9 \quad \tau_{TOT} = \tau_{EC} + \tau_D, \text{ (Eq. 3)}$$

10 From TOM we get the EC mass surface density ($\mu\text{g cm}^{-2}$). Thus, we can write τ_{EC} as the product of the
 11 EC mass surface density on the filter and an effective material specific mass absorption cross section
 12 $\text{MAC}_{\text{eff,EC}}$ of BC that includes the multiple scattering enhancement of the filter, which is applicable for
 13 our measurements and not necessarily as universal MAC values. Typically, MAC values are reported
 14 in units of $\text{m}^2 \text{g}^{-1}$.

15 **2.3 Laboratory tests**

16 A series of laboratory tests using the OCEC-analyzer and the PSAP combination were conducted before
 17 initiating analysis of the field samples. For this purpose, the following filter sets were created:

- 18 1. A set of filter samples (n=36) with different amounts of BC. Two types of soot (BC) were used
 19 and each was mixed (a small amount of soot not weighed) with MQ water and a small amount
 20 of ethanol (to enable mixing of the BC particles in the liquid) in an ultra-sonic bath. One soot
 21 type was collected by chimney cleaners in Helsinki, Finland, originating from oil-based
 22 combustion, and has been used previously in soot on snow experiments (Svensson et al., 2016).
 23 The second type was a product from NIST (National Institute of Standards and Technology),
 24 which consists of diesel particle matter from industrial forklifts, NIST-2975. From the BC stock
 25 solutions, different amounts of solution were taken out and diluted with additional water for the
 26 same total volume of filtrate (ca. 0.5 L liquid). The newly created mixture solution was
 27 thereafter filtered using the same filter procedure as the ambient snow samples (described in
 28 2.1.1).
- 29 2. The second set of filters (n=16) generated contained mineral dust only. Analogous to the soot
 30 mixtures, two types of mineral were used. The first mineral was SiC, (manufactured by
 31 Carborundum), mesh nr. 1200, corresponding to particles approximately $< 1 \mu\text{m}$ in diameter
 32 (Manufacturer). It is light grey with hints of blue in color and the amount of SiC added to the

1 MQ water was measured using a digital scale (resolution of 10 μg) before filtration. With the
2 known concentration of the mixture, we observed how much of the weighed mineral was
3 deposited on the filter during filtration to estimate losses. By comparing the whole filters before
4 and after filtration gravimetrically, these tests showed that 10 % or less of the mineral was lost
5 during filtering. The second type of mineral consisted of stone crush from a site in Stockholm,
6 Ulriksdal, likely to be mainly granite. A sieve mesh nr. 400 was used for this material, which
7 corresponds to mineral particles of approximately $< 38 \mu\text{m}$ in diameter. Filters were prepared
8 according to the procedure given above for the other mineral (SiC).

- 9 3. The last set of laboratory solutions made contained various mixtures of SiC mineral and
10 chimney soot ($n=30$). These filters were treated in the same way as described above, with a soot
11 stock solution and a mineral weighed solution being mixed into one solution.

12 The procedure to analyze all three sets of filters samples was identical. After the filter substrates had
13 dried, one punch (1 cm^2) from the filter was put into the PSAP instrument to measure the transmission
14 across the filter in relation to a blank filter. This punch was taken for analyses of OC and EC content
15 using the OCEC-analyzer. After the TOM, and removal of the carbonaceous particles, this filter punch
16 was again analyzed in the PSAP. Hence, we acquired the transmission through the filter before heating
17 and after heating in comparison to a blank filter. We did tests where the same filter punch was used in
18 the PSAP instrument as well as the OCEC-analyzer, and compared this to identical samples that were
19 used only in each instruments. Both procedures provided the same result. Furthermore, extensive tests
20 were carried out using blank filters that had been subject to filtering of MQ water and treated the same
21 way as prepared samples and the ambient snow samples. No measurable EC could be detected on these
22 filters. It should be noted that part of the second set of the laboratory filters (stone crush mineral) were
23 analyzed with a different, but identical, PSAP and OCEC-analyzer at a different laboratory (Stockholm
24 University).

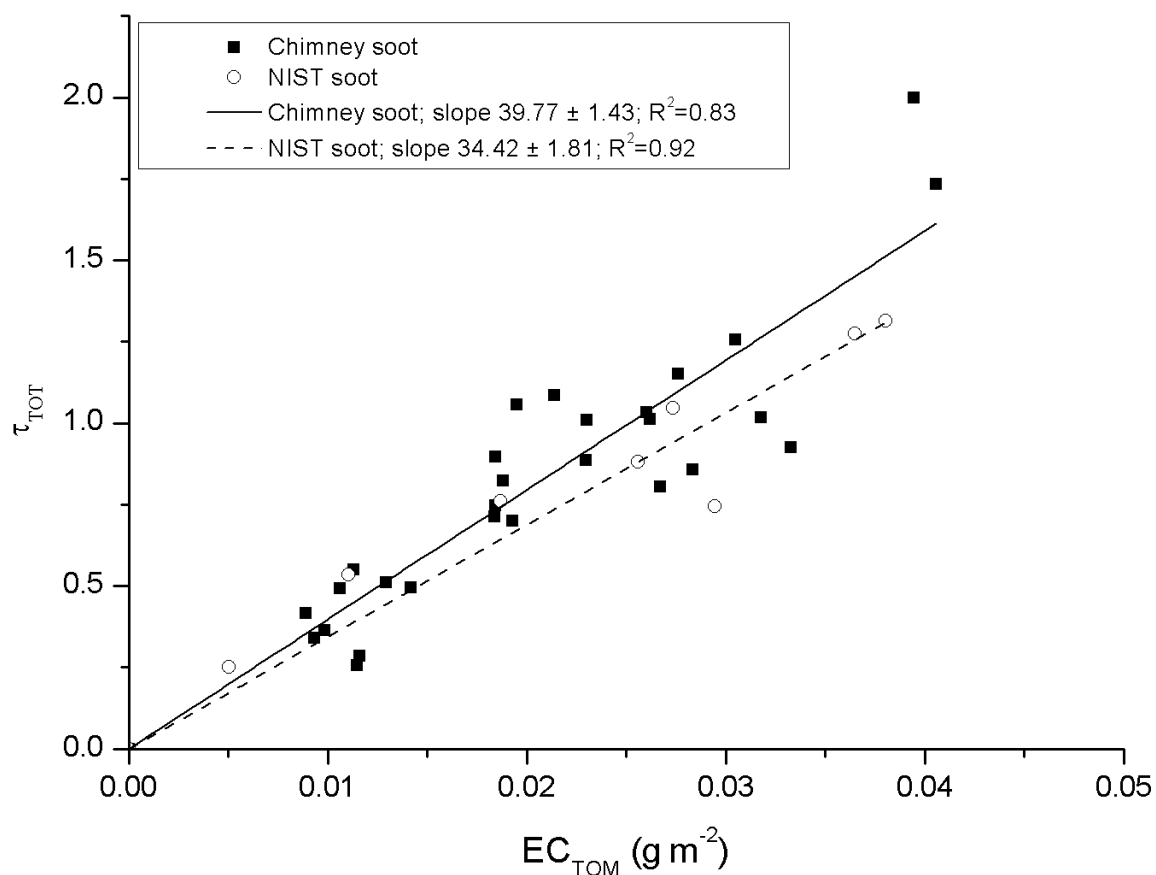
25 3. Results and discussion

26 3.1 Laboratory samples

27 The change in optical depth as a function of analyzed EC using our two standard types of BC particles
28 (filter set nr. 1) is shown in Figure 3. Both materials behave optically similar and the slopes are within
29 15 % of each other, with chimney soot having a slope of $39.8 \pm 1.54 \text{ m}^2 \text{ g}^{-1}$ and NIST soot 34.4 ± 1.8
30 $\text{m}^2 \text{ g}^{-1}$ (fits have been set to a fixed intercept at 0; \pm refers to standard error of slope). Previous studies
31 of atmospheric airborne BC aerosol and its MAC with different filter-based absorption photometers are
32 numerous, while reported MAC values for BC in snow are very sparse. The MAC value of BC is
33 dependent on many factors, such as particle size, density, and refractive index, mixing state (i.e.
34 coating). Reported airborne BC MAC values are lower than what we found for the two soot standards

1 (which were mixed in liquid solution to simulate similar conditions as for our ambient snow samples).
 2 However, the MAC of air sample usually takes into account the multiple-scattering correction factor
 3 (C_{ref}). For example for the commonly used aethalometer, its optical depth is divided by a C_{ref} in the
 4 range of 2.8-4.3 (Collaud Coen et al., 2010). If a C_{ref} of 5.2 was considered for our BC solution data,
 5 similar MAC values would be found (e.g. Bond et al. (2013) reports freshly-generated BC with a MAC
 6 of $7.5 \pm 1.2 \text{ m}^2 \text{ g}^{-1}$ at $\lambda = 550 \text{ nm}$). However, for our data set we have chosen not to take any C_{ref} into
 7 account as our samples are liquid instead of air based, and currently no C_{ref} exists for liquid samples.

8

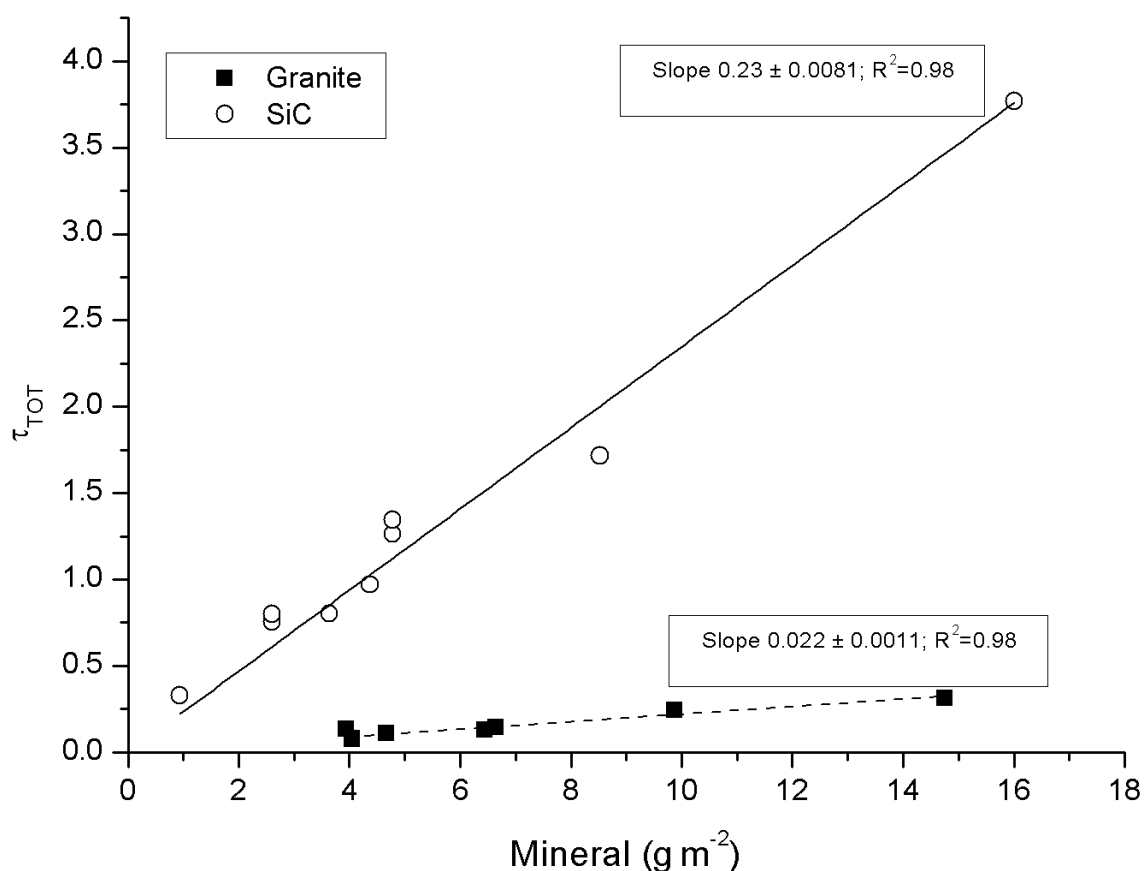


9

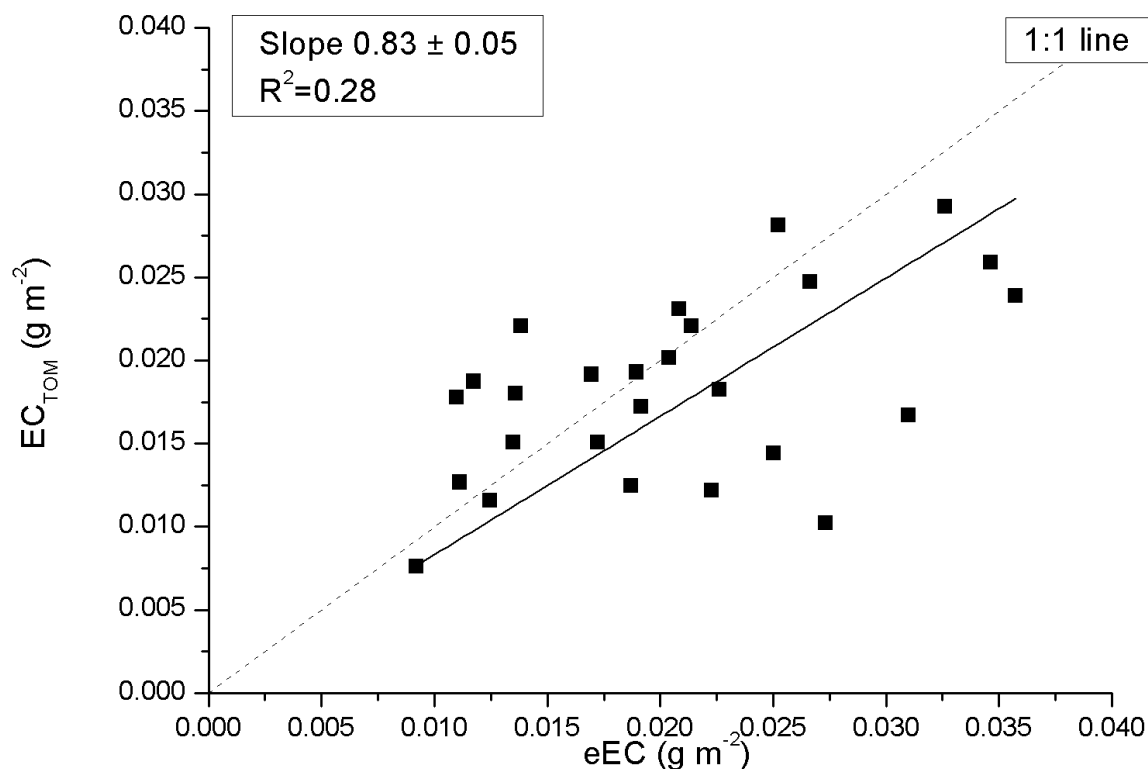
10 Figure 3. Comparison of the optical depth (at $\lambda=526 \text{ nm}$) by Chimney and NIST soot as function of
 11 analyzed EC density by the OCEC-analyzer.

12 Figure 4 shows results analogous to Figure 3, but for the two mineral aerosol solutions (filter set nr. 2).
 13 The slope of the optical depth of SiC versus measured SiC amount is more than a factor of one hundred
 14 smaller ($0.23 \pm 0.008 \text{ m}^2 \text{ g}^{-1}$) than the slopes for our BC standards. This is consistent with previously
 15 reported results for airborne mineral dust (e.g. Hansen et al., 1993). The stone crush material, an
 16 essentially white powder, yielded an even smaller slope of $0.02 \pm 0.001 \text{ m}^2 \text{ g}^{-1}$. Clearly, the slopes, or
 17 the MAC, for the mineral particles are very composition specific. For a few ($n=5$) of the mineral aerosol

1 samples the optical depth was measured both before and after TOM. No EC was detected on these
 2 samples and no significant difference in τ could be observed before and after heating the sample, as one
 3 would expect since no BC was added to these filters.



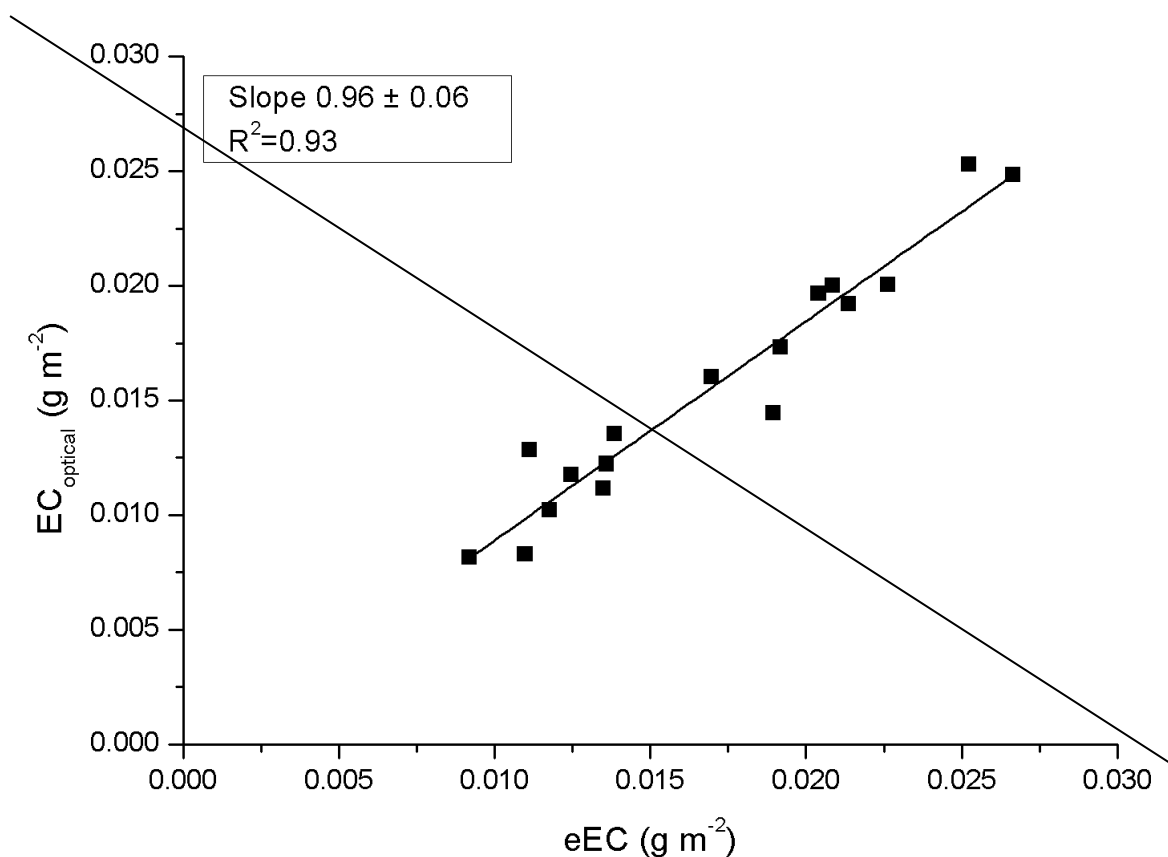
4
 5 Figure 4. The optical depth (at $\lambda=526$ nm) as a function of the amount of minerals present on the filter.
 6 From the analysis of chimney and NIST soot (Fig. 3) and SiC and stone crush dust (Fig. 4) the
 7 experiments were extended to comprise mixtures of soot and dust. Using the MAC of chimney soot
 8 (see Fig. 3), we estimate the EC content of the third set of filters, containing a mixture of SiC and
 9 chimney soot. The estimated EC (eEC) is based on the difference between the optical thickness before
 10 TOM analysis (τ_{TOT}) and the optical thickness after the analysis (τ_D). eEC is then compared to the
 11 amount of EC obtained in TOM, for the same filters. This comparison is presented in Figure 5. The data
 12 are rather scattered, but the slope of the linear regression is within 17 % of the 1:1 line. **The scatter seen**
 13 **in Figure 5 is due to the difference in the detection techniques (optical vs. TOM). The observed scatter**
 14 **in Figure 5 could also be related to the fact that BC is mixed with SiC. Nevertheless, Hence** it shows
 15 that EC can be reproduced reasonably well based on the PSAP measurement even for a mixture of BC
 16 and minerals.



1

2 Figure 5. EC amount observed by the TOM (EC_{TOM}) for Chimney soot and SiC mixtures as a function
 3 of estimated EC (eEC), using a PSAP optical depth signal before and after heating the filter and using
 4 the MAC_{eff,EC} of 39.8 m² g⁻¹ from Figure 3.

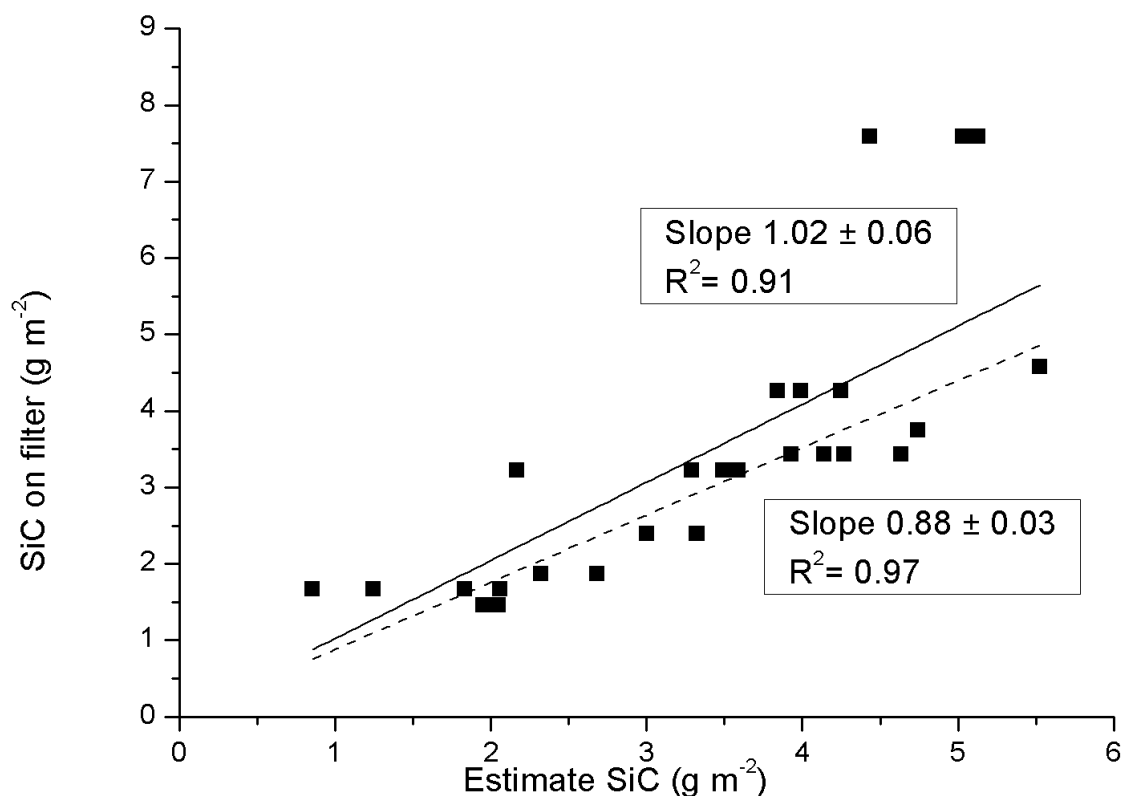
5 In the context of this work it is further useful to compare our eEC content with the optical EC reported
 6 by the OCEC analyzer. This comparison is presented in Figure 6, again for the third set of filters
 7 (Chimney soot+SiC). As observed, the EC amounts derived by two optically different methods show a
 8 consistent relation with nearly a slope of one. The good agreement between the two optically derived
 9 EC values suggests that much of the scatter seen in Figure 5 is due to the difference in the detection
 10 techniques (optical vs. TOM). The observed scatter in Figure 5 could also be related to the fact that BC
 11 is mixed with SiC.



1

2 ~~Figure 6. Comparison between the optically measurement of reported EC by the OCEC analyzer and~~
 3 ~~the derived EC surface amount on the substrate (using PSAP data and the relation in Figure 3). The data~~
 4 ~~is for filters containing mixtures of Chimney soot and SiC.~~

5 In addition to chimney soot, the mineral SiC is the second absorbing component on the third set of
 6 filters. In Figure 76 the optically estimated SiC content, based on the SiC slope in Figure 4 and τ_D is
 7 compared to the known weighed amount of SiC before adding it to the liquid. Similarly, as in Figure 5,
 8 there is some scatter in the data, but the overall pattern indicates a consistency with a reliable optical
 9 measurement. Two slopes presented, one including all of the data points (slope 1.02), and the second
 10 slope (0.88) excluding three data points with weighed SiC amounts exceeding 7.5 g m⁻².



1

2 Figure 76. Comparison between the weighed SiC amounts added to the water and the optically derived
 3 SiC density on the substrate. The data is for Chimney soot and SiC mixtures, with two alternative slopes;
 4 one containing all data points (1.02), and one excluding three data point in the top right of graph (0.88).

5 Based on the relations established for EC and SiC individually in figures 3 and 4, respectively, it is
 6 possible to retrieve their separate concentrations from a mixture based on the change in filter
 7 transmission before and after heating the filter. The consistent results from these laboratory tests gives
 8 confidence in applying this method on our ambient samples from India and Finland.

9 3.2 Ambient snow samples

10 3.2.1 EC in snow

11 In all of the snow pits from Sunderdhunga a distinct layer with concentrated impurities was observed.
 12 These impurity layers always had the highest EC concentrations (exceeding 300 $\mu\text{g L}^{-1}$) of each pit
 13 (Table 1). For some of the samples from Sunderdhunga taken from the impurity concentrated layers,
 14 the substrates were actually too loaded with material and quantitative impurity values could not be
 15 determined (by not having an initial transmission value). Excluding these heavy impurity layers, the
 16 average and median EC concentration for the other snow samples were 141.3 and 101.9 $\mu\text{g L}^{-1}$,
 17 respectively. Surface samples taken above 4900 m a.s.l. had EC concentrations in the range of 13.2-

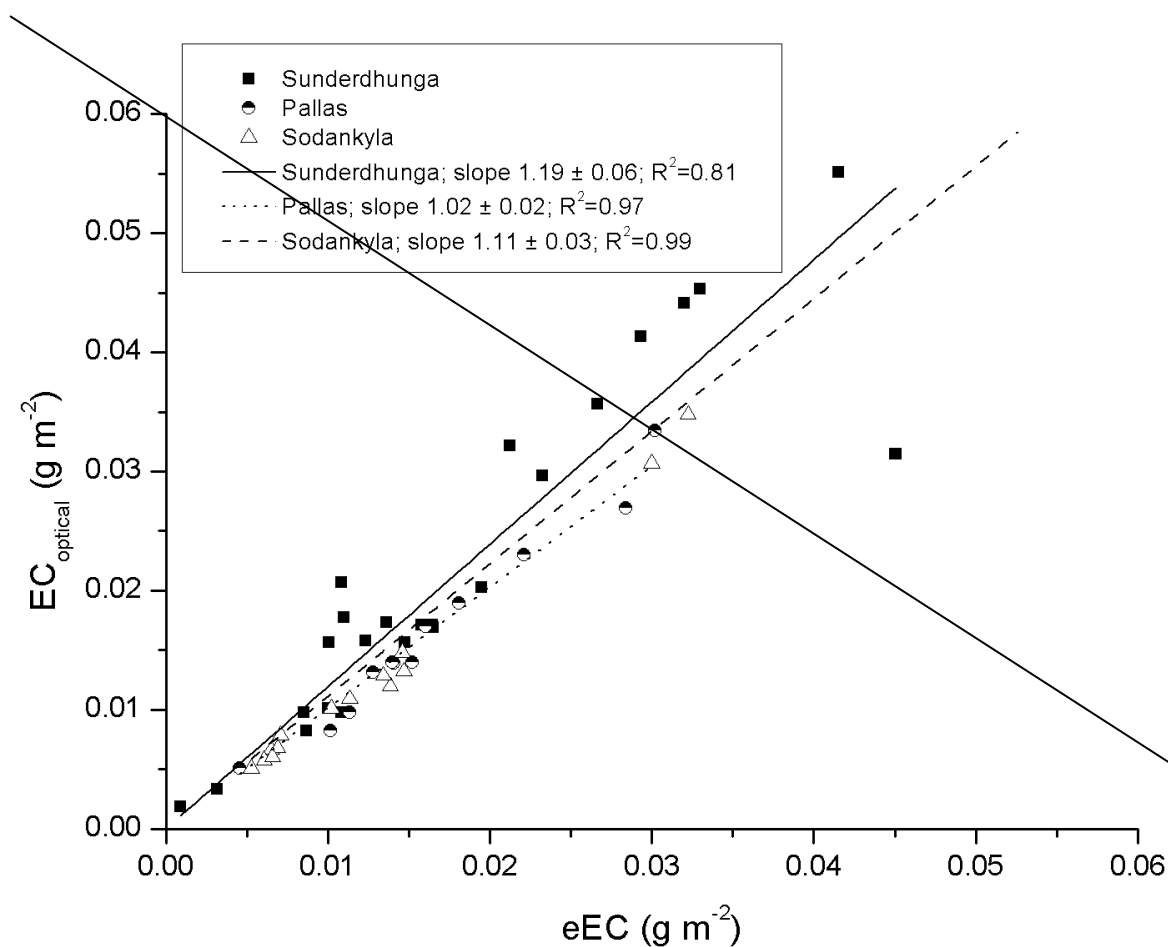
1 65.7 $\mu\text{g L}^{-1}$. Consisting of relatively fresh snow, fallen during the previous days (or weeks), these
2 surface samples contained LAI mostly originate from the post-monsoon season.

3 Previous studies of BC in snow and ice from the Himalaya have shown seasonal variation. At Mera
4 glacier in Nepal Ginot et al. (2014) showed that BC concentrations peak during the pre-monsoon in a
5 shallow ice core. From the same glacier, Kaspari et al. (2014) observed similar seasonal peaks in BC
6 concentration in snow and firn samples taken above the equilibrium line altitude, where the snow had
7 not undergone any significant summer melt. Noteworthy, dust did not show the same strong seasonality
8 as BC in their studies (Ginot et al., 2014; Kaspari et al., 2014).

9 Measurements of BC in snow taken closest to Sunderdhunga, reported in the literature, are from about
10 140 km east-north-east (78° heading), at a higher altitude between 5780-6080 m a.s.l. Gathered in the
11 surface snow of Namunani glacier Xu et al. (2006) reported low EC concentrations in the range of 0.3-
12 9.7 $\mu\text{g L}^{-1}$. The difference between Sunderdhunga and Namunani can probably be attributed to the
13 expected high spatial variability of BC in snow in the area. The difference in sampling altitude and
14 different measurement techniques to determine the EC likely plays a role as well (Xu et al. used a two-
15 step heating-gas chromatography, similar to method of Lavanchy et al.). The difference could also
16 possibly be explained by the geographical location, with Namunani located on the northern flank of the
17 Himalaya, and it is on the leeward side of the main sources of LAI to the south. Furthermore, it is not
18 explicitly stated in Xu et al. during which season snow samples were collected, which likewise would
19 affect EC concentrations.

20 For reference, the EC concentration in the surface snow from the Finnish Arctic were in the range of
21 6.2-102 $\mu\text{g L}^{-1}$. Samples from Pallas had an average and median of 40.0 and 31.0 $\mu\text{g L}^{-1}$, respectively,
22 whereas the samples from Sodankylä had an average of 23.7 $\mu\text{g L}^{-1}$ and median of 13.1 $\mu\text{g L}^{-1}$. The
23 higher concentration observed in Pallas might result from the fact that the majority of samples was
24 taken later in the snow season compared to Sodankylä samples and EC has likely concentrated in the
25 surface snow later in the season (e.g. Svensson et al., 2013). On a larger scale, the concentrations are in
26 the same magnitude as previous measurements of EC in snow from the European Arctic (Forsström et
27 al., 2013; Meinander et al., 2013; Svensson et al., 2013).

28 ~~Our snow samples EC content is further compared in Figure 8, where the estimated EC content based~~
29 ~~on the optical depth measurement is plotted against the optical EC output from the OCEC analyzer. The~~
30 ~~snow data presented in Figure 8 indicate the same relation between the two optical methods as presented~~
31 ~~in Figure 6 for the standard soot. That is, slopes near 1:1 line, namely 1.19, 1.02, and 1.11 for~~
32 ~~Sunderdhunga, Pallas, and Sodankylä samples, respectively. Hence, there is a strong consistency~~
33 ~~between the two optical approaches in the interpretation of the change in τ before and after the substrate~~
34 ~~has been analyzed with the EUSAAR 2 thermal protocol.~~

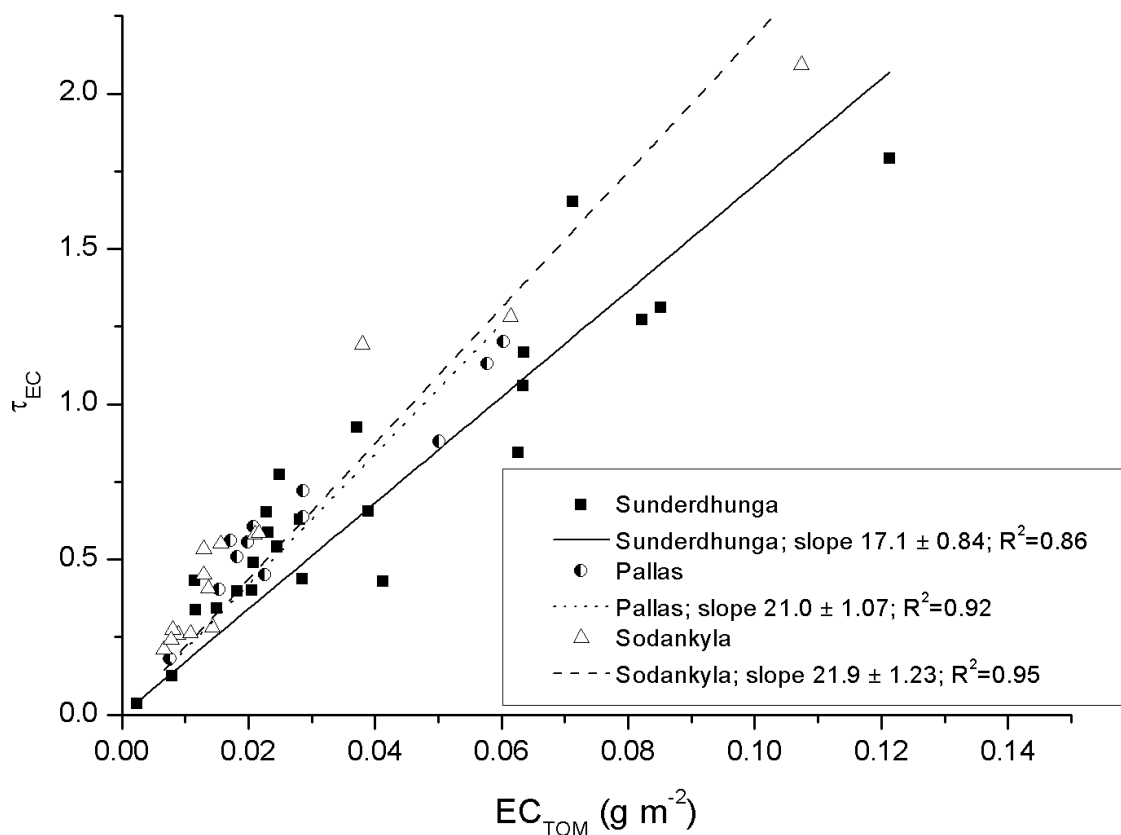


1

2 Figure 8. Comparison between the optical EC content given by the OCEC analyzer and estimated EC
 3 (eEC) content using a PSAP and a $MAC_{eff,EC}$ of $39.8 \text{ m}^2 \text{ g}^{-1}$, for the Arctic and Himalayan samples.

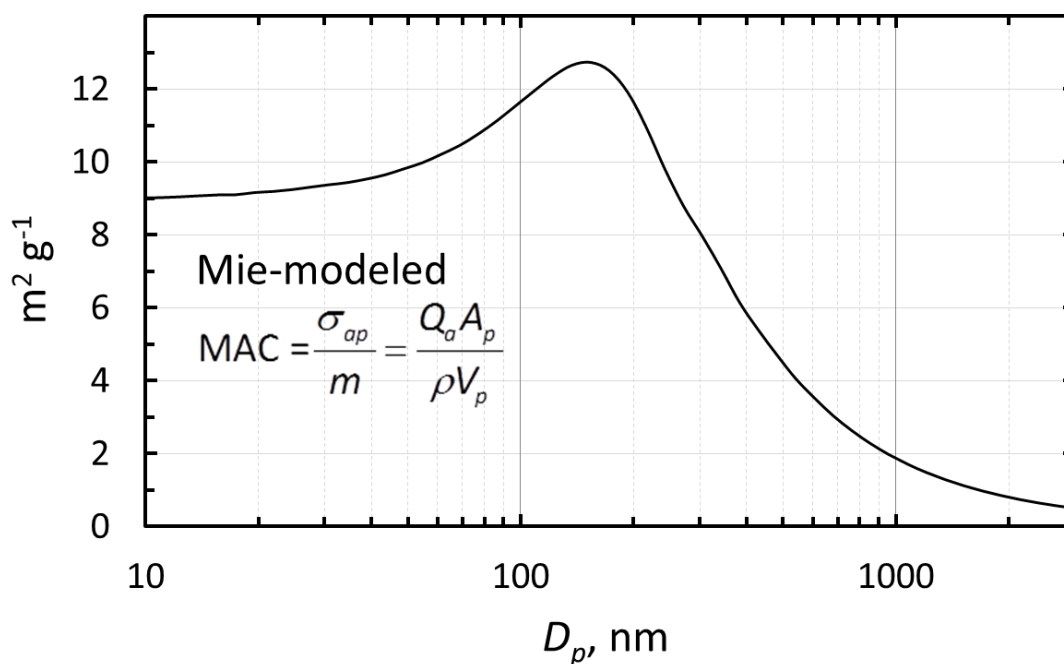
4 Although the EC content determined by the optical method of the TOM and the eEC content based on
 5 the PSAP and a MAC value (Figure 3) agree well, there is a significant difference in the site specific
 6 derived MAC values there is a significant difference. In Figure 97 the optical depth of EC (τ_{EC}) is plotted
 7 as a function of the analyzed EC (with TOM) for all of the snow samples. The slopes for the three
 8 sampling sites are 21.0, 21.9 and $17.1 \text{ m}^2 \text{ g}^{-1}$ (Pallas, Sodankylä, and Sunderdhunga, respectively).
 9 These values are around half of what the laboratory standard BC tests show (Fig. 3), indicating a smaller
 10 absorption efficiency for the EC particles originating from the snow compared to the laboratory
 11 particles. This is unexpected, as any non-EC absorbing material or even scattering particles mixed with
 12 EC would tend to increase the MAC value compared to pure BC particles (e.g. Cappa et al., 2012; Bond
 13 et al., 2013). In our case, we would expect the MAC to be greater for our snow originating EC particles.
 14 A consequence of a lower MAC for the snow EC particles could be that the snow albedo reduction
 15 caused by the EC is inaccurate since the EC particles have less absorbing efficiency. Schwarz et al.
 16 (2013) previously reported a lower MAC value for BC particles in the snow compared to airborne BC
 17 particles due to a difference in the measured mean size. The BC particles from the snow were observed

- 1 to be larger compared to airborne BC particles, explaining the decrease in MAC for the snow particles.
- 2 The authors further showed how the BC effect in snow albedo reduction is currently overestimated due
- 3 to the lower MAC for snow BC particles.



4
5 Figure 97. The optical depth τ_{EC} as function of the analyzed EC based on TOM, for the Arctic and
6 Himalayan samples.

7 In our case, if the laboratory generated BC consist of smaller particles compared to the snow samples
8 this could lead to a larger MAC value for the lab-standards. The size distribution of the BC particles in
9 the filters are unknown to us, but as suggested by the modelled MAC curve, presented in Figure 498,
10 this size dependence can play a role. The modelled MAC for theoretical BC particles demonstrates a
11 decrease in MAC with particle size, particularly for particles larger than about 130 nm. The absorption
12 efficiencies were calculated for $\lambda = 526\ nm$ by using the Mie code of Barber and Hill (1990) and for
13 BC we use the same complex refractive index of $1.85 - 0.71i$ that was used by Lack and Cappa (2010)
14 and a particle density of $1.7\ g\ cm^{-3}$.



1

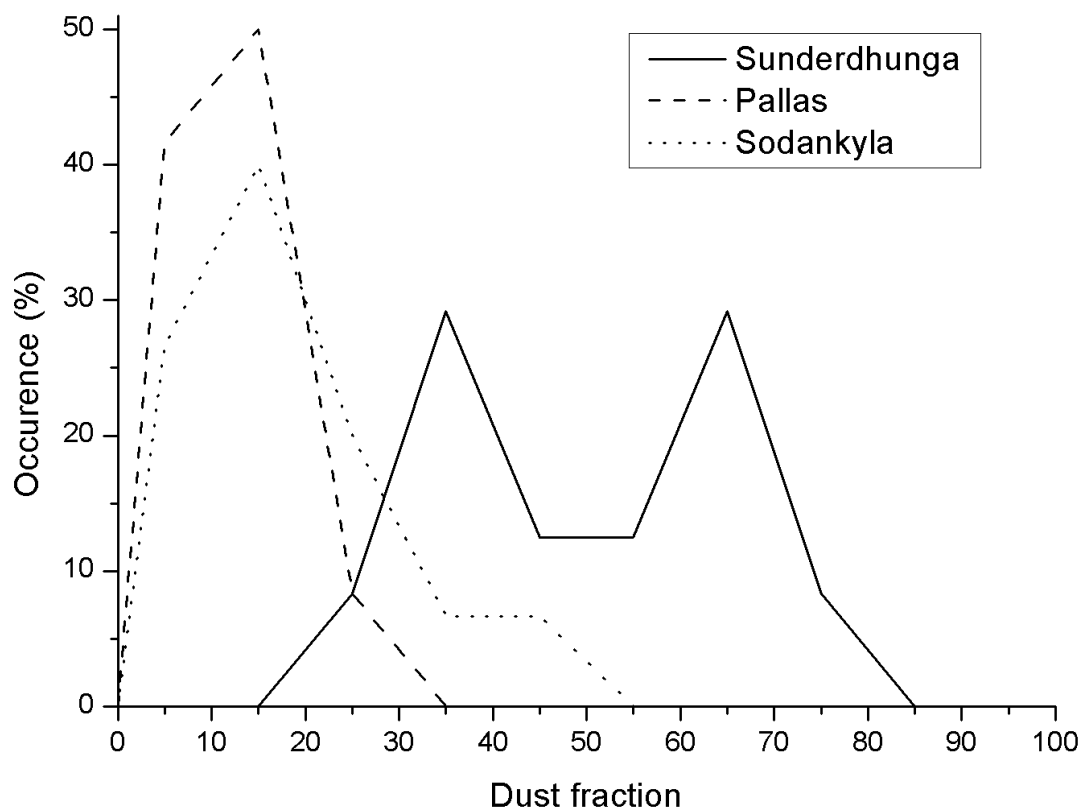
2 Figure 408. Modeled mass absorption coefficient (MAC) of single BC particles as a function of particle
 3 diameter at $\lambda = 526$ nm.

4 Another hypothesis is related to the fact that the samples are liquids and that the matrix is strongly light
 5 scattering and rather thick. It is likely that the liquid will embed the particles deeper into the filter than
 6 what is typical for air samples (e.g. Chen et al., 2004). In air and on filter surfaces, BC mixed with a
 7 scattering medium shows enhanced absorption. On the samples presented in Table 1, about 90 to 95%
 8 of the carbon is water insoluble organic carbon, whereas the laboratory BC was essentially free from
 9 OC. This difference could explain the lower MAC for the ambient samples if the net effect of the added
 10 OC actually made the BC less efficient absorber in this particular matrix. Further tests are required,
 11 however, to confirm this hypothesis.

12 3.2.2 Dust fraction of LAI in snow

13 Because the ambient mineral dust MAC value is unknown for our snow samples, it is not possible to
 14 use the SiC or stone crush MAC values to estimate the dust content on the filters. Instead, we use the
 15 fraction of minerals (f_D) expressed in percent of the total optical thickness, $\left(\frac{\tau_D}{\tau_{TOT}} 100 \%\right)$ to estimate
 16 the mineral aerosol contribution to the filter absorption (at $\lambda = 526$ nm). In our data set, there is a
 17 systematic difference between the two Arctic sites and the Himalaya site (Fig. 419). For Pallas and
 18 Sodankylä f_D is typically less than 20 %, whereas for Sunderdhunga f_D is typically much greater than
 19 that, with modes at 35 and 65 %. For the Arctic, the values are broadly in line with previous estimates
 20 on the amount of light absorption caused by LAI other than BC, i.e. 30-50 % (e.g. Doherty et al., 2010).

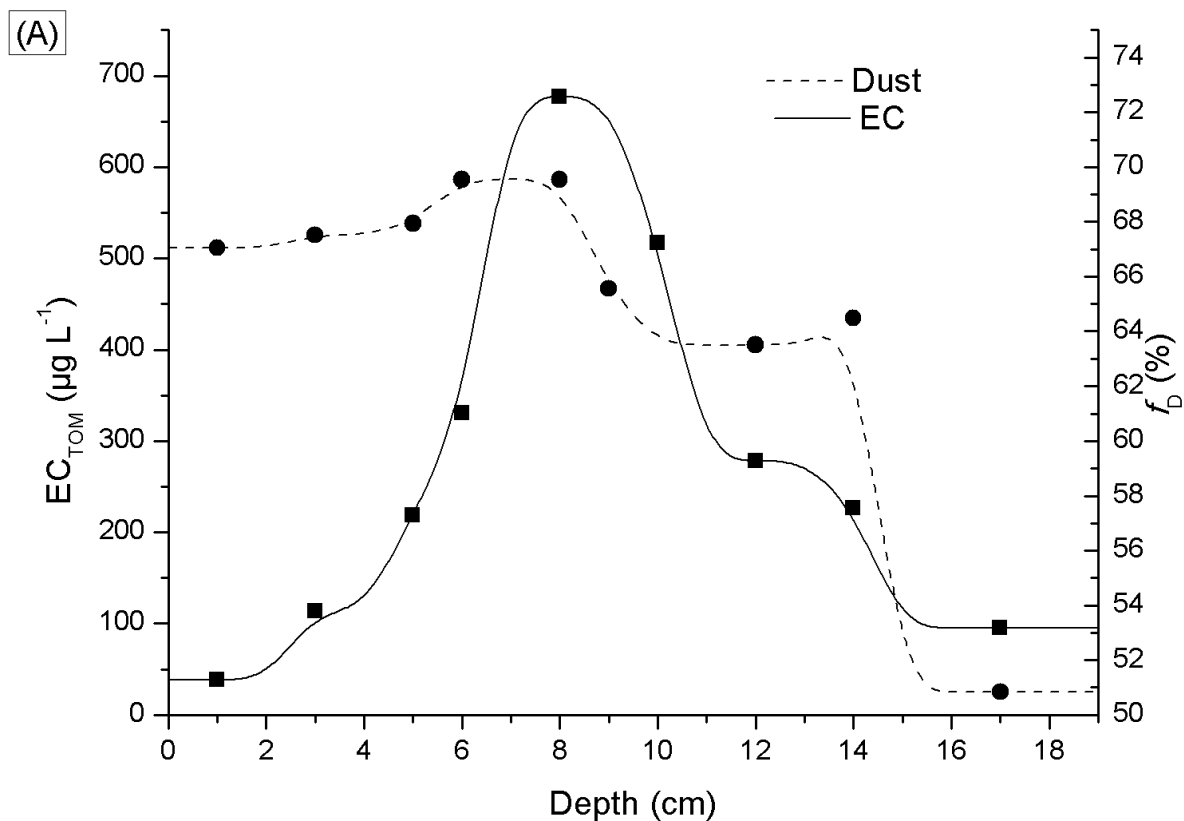
1 Studies from the Nepalese Himalaya concluded that dust may be responsible for about 40 % of the snow
 2 albedo reduction (Kaspari et al., 2014). Similarly, Qu et al. (2014) observed that the contribution of dust
 3 to albedo reduction can reach as much as 56 % on a glacier in the Tibetan plateau. Our dust estimate,
 4 as a fraction of the optical depth of LAI on the filter, shows similar results or an even greater fraction
 5 of dust than these previous studies, highlighting the importance of dust (see also Fig. 12A) causing
 6 albedo reduction in this region of the Himalaya.



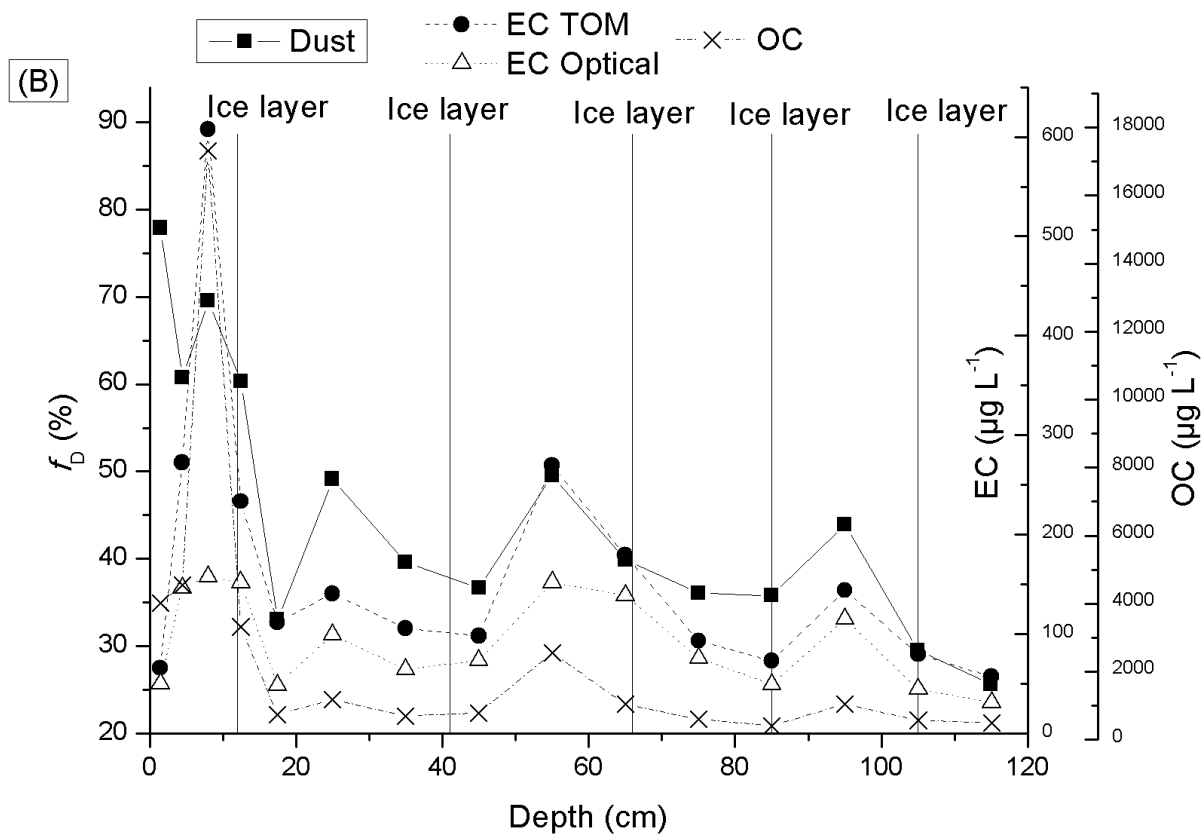
7
 8 Figure 119. Frequency of the occurrence of dust optical thickness fractions at the three sampling sites

9 3.2.3 Vertical distribution of LAI in Sunderdhunga

10 An average of the vertical profiles from pits C, D, and E are presented for EC and f_D in Figure 120A.



1



2

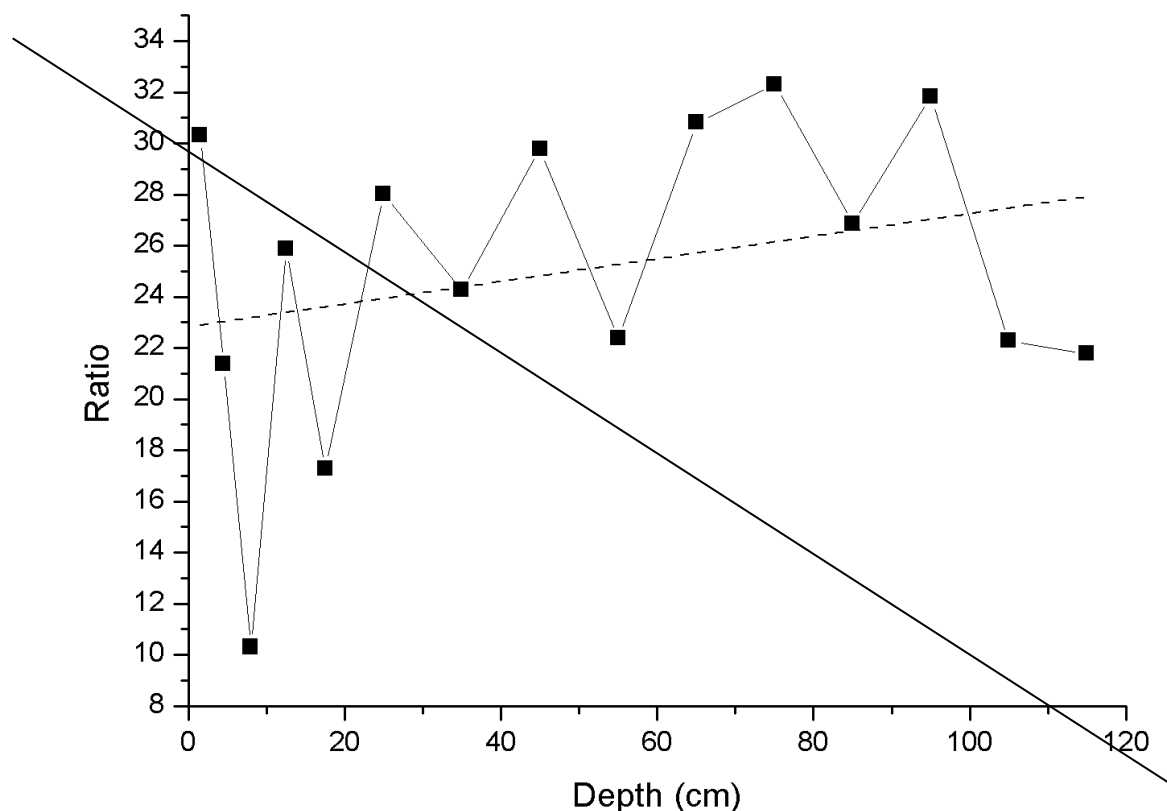
1 Figure 1210. (A) Profile displaying average EC concentration and dust fraction from snow pits C and
2 D (Durga Kot glacier), and snow pit E (Bhanolti glacier); (B) Complete vertical profile E, taken at
3 Bhanolti glacier.

4 The variables plotted in Figure 120B display layers of enhanced amounts of both dust and EC, located
5 between ice layers, and additionally high values at the top of the pit above the first ice layer. These
6 layers are interpreted as indicators for seasonal variation at this location, with alternating melt and
7 refreezing periods marked by the ice layers. Since the ice layers and the enhancements in LAI are
8 interleaved it suggest that the impurities were deposited on the glacier mainly in-between the melt and
9 refreeze periods. In addition, the melting seems to take place in a relative shallow layer at the surface
10 and does not protrude deeply, which may cause the annual layers to mix (Doherty et al., 2013). The
11 observed variation in EC and dust values could correspond to the findings of Ginot et al. (2014) and
12 Kaspari et al. (2014) who showed annually peaking BC concentrations in the pre-monsoon in
13 Himalayan ice cores. However, for instance, between the ice layers at ca. 65 and 85 cm, no clear peak
14 is observed in EC or dust values (Fig. 120B), which could either indicate that no peak occurred during
15 that particular year, or an ice layer formed at ca. 65 cm in the middle of the year, similarly as potentially
16 at ca. 105 cm.

17 The snow pit covers potentially five years of snow accumulation which is certainly a too short time
18 period to make any conclusions on a temporal trend of LAI variations at the site. However, an evident
19 increase in LAI is present, especially in the top 20 cm. Due to the time span of the snow pit we cannot
20 know for certain whether this increase presents a short term pollution event or indicates increasing LAI
21 at the site over a longer time period. We have two hypothesis for the observed increase in EC
22 concentrations and the fraction of dust occurring in the top layer of the snow pit. The higher values may
23 be a consequence of increased ambient EC and dust concentrations in the area, causing increased dry
24 and wet deposition fluxes of these impurities to the glacier, even when assuming constant precipitation.
25 Moreover, as it is f_D that increases, the deposition of dust would have had to increase proportionally
26 more than EC and OC. This could be a result from larger areas in the region being free of snow or
27 changes in the wind characteristics (e.g. stronger winds and/or change in direction). On the other hand,
28 local changes in the net snow mass balance due to a larger fraction of the snow being sublimated in the
29 time period covered by the top 20 cm in comparison to the deeper layers, may partly explain the
30 increased EC and dust absorption values at the top of the pit. Both these basic scenarios can be in effect
31 at the same time.

32 Interestingly, while the EC and OC concentrations and f_D are peaking at the top of the snow pit and
33 potentially decrease very slightly towards the bottom of the snow pit, the absorbing efficiency of EC
34 seems to be decrease towards the top of the snow pit. We illustrate this in Figure 13 by plotting the ratio
35 between the optical EC from the OCEC analyzer and the analyzed EC based on TOM, and scale this

1 ratio with the MAC value of 39.8 derived in Figure 3. While the EC concentrations in the snow are the
 2 highest at the top of the pit, it appears that at the same time this EC is a less potent light absorber per
 3 unit mass (Fig. 13) than in deeper snow layers. This observation is rather hypothetical, and it needs to
 4 be further explored.



5
 6 Figure 13. The ratio between the optical EC content and analyzed EC content (TOM method) as
 7 measured by the OCEC analyzer using the EUSAAR 2 thermal protocol. The ratio is scaled by the
 8 effective MAC value of $39.78 \text{ m}^2 \text{ g}^{-1}$ derived in Figure 3.

9 4. Conclusions

10 Here, first observations of LAI in snow originating from two glaciers in the Indian Himalaya are
 11 presented with a method not used widely before to determine LAI in snow. Consisting of a custom built
 12 PSAP and an OCEC-analyzer, the attenuation of light is studied on quartz filters, providing estimates
 13 on the fraction of light-absorbance caused by non-EC constituents in LAI. Himalayan data display a
 14 much greater light-absorbance by dust in the LAI compared to filter samples originating from the
 15 seasonal snowpack of Arctic Finland. The role of dust in reducing the snow albedo in this part of
 16 Himalayan glaciers needs to be further evaluated, as our results suggest that it might be the dominating
 17 LAI in the snow. Our measurements further reveal that the optical properties of EC are different for
 18 laboratory generated soot compared to EC deposited on snow. Our finding of a MAC value of about

1 half of the laboratory EC for the ambient EC particles, it can have implications for the snow albedo
 2 reduction caused by EC. Over the last approximately five year period in the Himalaya, EC
 3 concentrations in the snow display signs of increase in the top part of the snow pit compared to deeper
 4 layers, while at the same time its light absorbing potential suggests a decrease towards the highest EC-
 5 laden layers. Consequently, a Additional work on the optical properties of EC in snow are needed to
 6 enable more accurate estimates of albedo reduction caused by EC in snow, both spatially and
 7 temporally. This should be done by measuring the EC particles light-absorption properties while in the
 8 snow since the ambient conditions can be different than laboratory settings.

9 **Acknowledgments**

10 This work has been supported by the Academy of Finland projects: Absorbing Aerosols and Fate of
 11 Indian Glaciers (AAFIG; project number 268004) and Greenhouse gas, aerosol and albedo variations
 12 in the changing Arctic” (project number 269095), and Novel Assessment of Black Carbon in the
 13 Eurasian Arctic: From Historical Concentrations and Sources to Future Climate Impacts (NABCEA
 14 (project number 296302). The Academy of Finland Center of Excellence program (project number
 15 272041), as well as the Nordic research and innovation initiative Cryosphere-Atmosphere Interactions
 16 in a Changing Arctic Climate have also supported this work. Jonas Svensson is thankful for the support
 17 from Svenska kulturfonden. We would like to thank the providers of the soot Consti Taloteknikka, and
 18 Göran Lidén at SU luftlab for the mineral samples. The ACES department at Stockholm University, is
 19 part of the Bolin centre for climate research. Finally we would like to thank the participants of the
 20 AAFIG 2015 expedition, including Sherpas and guides from Real adventure, for their work during the
 21 expedition.

22 **References**

- 23 AMAP: The Impact of Black Carbon on Arctic Climate. Arctic Monitoring and Assessment Programme
 24 (AMAP), Oslo, Norway, 72 pp, 2011.
- 25 Aoki, T., Motoyoshi, H., Kodama, Y., Yasunari, T. J., Sugiura, K., and Kobayashi, H.: Atmospheric
 26 aerosol deposition on snow surfaces and its effect on albedo. *SOLA*, 2, 13–16, doi: 10.2151/sola.2006-
 27 004, 2006.
- 28 Barber, P. W. and Hill, S. C.: Light scattering by particles: Computational methods, World Scientific
 29 Publishing, Singapore, 1990.
- 30 Birch, M. E., and Cary R. A.: Elemental carbon-based method for monitoring occupational exposures,
 31 to particulate diesel exhaust, *Aerosol. Sci. Technol.*, 25, 221– 241, 1996.
- 32 Bolch, T., Kulkarni, A., Käab, A., Huggel, C., Paul, F., Cogley, J. G., Frey, H., Kargel, J. S., Fujita, K.,
 33 Scheel, M., Bajracharya, S., and Stoffel, M.: The State and Fate of Himalayan Glaciers, *Science*, 336,
 34 310–314, doi:10.1126/science.1215828, 2012.
- 35 Bond, T. C., Anderson, T. L., and Campbell, D.: Calibration and Intercomparison of Filter-Based
 36 Measurements of Visible Light Absorption by Aerosols, *Aerosol Sci. Technol.* 30:582–600, 1999.
- 37 Bond, T. C., Doherty, S. J., Fahey, D. W., Forster, P. M., Berntsen, T., DeAngelo, B. J., Flanner, M. G.,
 38 Ghan, S., Kärcher, B., Koch, D., Kinne, S., Kondo, Y., Quinn, P. K., Sarofim, M. F., Schultz, M. G.,
 39 Schulz, M., Venkataraman, C., Zhang, H., Zhang, S., Bellouin, N., Guttikunda, S. K., Hopke, P. K.,
 40 Jacobson, M. Z., Kaiser, J. W., Klimont, Z., Lohmann, U., Schwarz, J. P., Shindell, D., Storelvmo, T.,

- 1 Warren, S. G., and Zender, C.S.: Bounding the role of black carbon in the climate system: A scientific
2 assessment, *J. Geophys. Res. Atmos.*, 188, 5380–5552, doi: 10.1002/jgrd.50171, 2013.
- 3 Bond, T., Bhardwaj, E., Dong, R., Jogani, R., Jung, S., Roden, C., Streets, D. G., and Trautmann, N.:
4 Historical emissions of black and organic carbon aerosol from energy-related combustion, 1850–2000,
5 *Global Biogeochem. Cy.*, 21, doi:10.1029/2006GB002840, 2007.
- 6 Cachier, H., Bremond, M.P., and Buat-Ménard, P.: Determination of atmospheric soot carbon with a
7 simple thermal method, *Tellus Ser.B*, 41B, 379-390, 1989.
- 8 Cappa, C., Onasch, T., Massoli, P., Worsnop, D., Bates, T., Cross, E., Davidovits, P., Hakala, J.,
9 Hayden, K., Jobson, B., Kolesar, K., Lack, D., Lerner, B., Li, S., Mellon, D., Nuaaman, I., Olfert, J.,
10 Petäjä, T., Quinn, P., Song, C., Subramanian, R., Williams, E., and Zaveri, R.: Radiative absorption
11 enhancements due to the mixing state of atmospheric black carbon, *Science*, 337, 1078–1081,
12 doi:10.1126/science.1223447, 2012.
- 13 Cavalli, F., Viana, M., Yttri, K.E., Genberg, J., and Putaud, J.-P.: Toward a standardised thermal-optical
14 protocol for measuring atmospheric organic and elemental carbon: the EUSAAR protocol, *Atmos.*
15 *Meas. Tech.* 3, 79–89, doi:10.5194/amt-3-79-2010, 2010.
- 16 Chen, L.-W. A., Chow, J. C., Watson, J. G., Moosmüller, H., and Arnott, W. P.: Modeling reflectance
17 and transmittance of quartz-fiber filter samples containing elemental carbon particles: Implications for
18 thermal/optical analysis, *J. Aerosol Sci.*, 35, 765–780, 2004.
- 19 Chow, J. C., & Watson, J. G.: PM_{2.5} carbonate concentrations at regionally representative Interagency
20 monitoring of protected visual environment sites. *J. Geophys. Res.*, 107(D21), 8344,
21 doi:10.1029/2001JD000574, 2002.
- 22 Collaud Coen, M., Weingartner, E., Apituley, A., Ceburnis, D., Fierz-Schmidhauser, R., Flentje, H.,
23 Henzing, J. S., Jennings, S. G., Moerman, M., Petzold, A., Schmid, O. and Baltensperger, U.:
24 Minimizing light absorption measurement artifacts of the Aethalometer: evaluation of five correction
25 algorithms, *Atmos. Meas. Tech.*, 3, 457–474, 10.5194/amt-3-457-2010, 2010.
- 26 Doherty, S. J., Warren, S. G., Grenfell, T. C., Clarke, A. D., and Brandt, R. E.: Light-absorbing
27 impurities in Arctic snow, *Atmos. Chem. Phys.*, 10, 11647–11680, doi: 10.5194/acp-10-11647-2010,
28 2010.
- 29 Doherty, S. J., Grenfell, T. C., Forsström, S., Hegg, D. L., Brandt, R. E., and Warren, S. G.: Observed
30 vertical redistribution of black carbon and other insoluble light-absorbing particles in melting snow, *J.*
31 *Geophys. Res.*, 118, 1–17, doi:10.1002/jgrd.50235, 2013.
- 32 Doherty, S. J., D. A. Hegg, J. E. Johnson, P. K. Quinn, J. P. Schwarz, C. Dang, and Warren, S.G.:
33 Causes of variability in light absorption by particles in snow at sites in Idaho and Utah, *J. Geophys.*
34 *Res. Atmos.*, 121, 4751-4768, doi:10.1002/2015JD024375, 2016.
- 35 Dumont, M., Brun, E., Picard, G., Michou, M., Libois, Q., Petit, J.-R., Geyer, M., Morin, S., and Josse,
36 B.: Contribution of light-absorbing impurities in snow to Greenland's darkening since 2009, *Nat.*
37 *Geosci.*, 7, 509–512, doi:10.1038/ngeo2180, 2014.
- 38 Forsström, S., Ström, J., Pedersen, C. A., Isaksson, E., and Gerland, S.: Elemental carbon distribution
39 in Svalbard snow, *J. Geophys. Res. Atmos.*, 114, D19112, doi:10.1029/2008JD011480, 2009.
- 40 Forsström, S., Isaksson, E., Skeie, R. B., Ström, J., Pedersen, C. A., Hudson, S. R., Berntsen, T. K.,
41 Lihavainen, H., Godtliebsen, F., and Gerland, S.: Elemental carbon measurements in European Arctic
42 snow packs, *J. Geophys. Res. Atmos.*, 118, 13614–13627, doi:10.1002/2013JD019886, 2013.
- 43 Gautam R., Hsu, N. C., Lau, W. K.-M., and T. J. Yasunari, T. J.: Satellite observations of desert dust-
44 induced Himalayan snow darkening, *Geophys. Res. Lett.*, 40, 988–993, doi:10.1002/grl.50226, 2013.
- 45 Gertler, C.G., Puppala, S.P., Panday, A., Stumm, D., Shea, J.: Black carbon and the Himalayan
46 cryosphere: a review. *Atmos. Environ.* 125, 404–417, doi.org/10.1016/j.atmosenv.2015.08.078, 2016.
- 47 Ginot, P., Dumont, M., Lim, S., Patris, N., Taupin, J.-D., Wagnon, P., Gilbert, A., Arnaud, Y., Marinoni,
48 A., Bonasoni, P., and Laj, P.: A 10 year record of black carbon and dust from a Mera Peak ice core
49 (Nepal): variability and potential impact on melting of Himalayan glaciers, *The Cryosphere*, 8, 1479–
50 1496, doi:10.5194/tc-8-1479-2014, 2014.
- 51 Grenfell, T. C., Doherty, S. J., Clarke, A. D., and Warren, S. G.: Spectrophotometric determination of
52 absorptive impurities in snow, *Appl. Opt.*, 50(14), 2037–2048.
- 53 Hagler, G. S. W., Bergin, M. H., Smith, E. A., Dibb, J. E., Anderson, C., and Steig, E. J.: Particulate
54 and water-soluble carbon measured in recent snow at Summit, Greenland, *Geophys. Res. Lett.*, 34,
55 L16505, doi:10.1029/2007GL030110, 2007.

- 1 Hansen, A.D. A., Kapustin, V. N., Kopeikin, V. M., Gillette, D. A., and Bodhaine, B. A.: Optical
2 absorption by aerosol black carbon and dust in a desert region of central Asia, *Atmos. Environ., Part 4*,
3 27,4, 2527-2531, 1993
- 4 Hinds, W. C.: *Aerosol Technology*, Wiley-Interscience, 1999.
- 5 Hyvärinen, A.-P., Raatikainen, T., Brus, D., Komppula, M., Panwar, T. S., Hooda, R. K., Sharma, V.
6 P., and Lihavainen, H.: Effect of the summer monsoon on aerosols at two measurement stations in
7 Northern India – Part 1: PM and BC concentrations, *Atmos. Chem. Phys.*, 11, 8271-8282,
8 doi:10.5194/acp-11-8271-2011, 2011.
- 9 Immerzeel, W. W., van Beek, L. P. H., and Bierkens, M. F. P.: Climate Change Will Affect the Asian
10 Water Towers, *Science*, 328, 1382–1385, doi:10.1126/science.1183188, 2010.
- 11 Jankowski, N., Schmidl, C., Marr, I. L., Bauer, H., and Puxbaum, H.: Comparison of methods for the
12 quantification of carbonate carbon in atmospheric PM₁₀ aerosol samples, *Atmos. Environ.*, 42, 8055–
13 8064, 2008.
- 14 Karanasiou, A., Diapouli, E., Cavalli, F., Eleftheriadis, K., Viana, M., Alastuey, A., Querol, X., and
15 Reche, C.: On the quantification of atmospheric carbonate carbon by thermal/optical analysis protocols,
16 *Atmos. Meas. Tech.*, 4, 2409–2419, doi:10.5194/amt4-2409-2011, 2011.
- 17 Kaspari, S., Painter, T. H., Gysel, M., Skiles, S. M., and Schwikowski, M.: Seasonal and elevational
18 variations of black carbon and dust in snow and ice in the Solu-Khumbu, Nepal and estimated radiative
19 forcings, *Atmos. Chem. Phys.*, 14, 8089–8103, doi:10.5194/acp-14-8089-2014, 2014.
- 20 Kääb, A., Berthier, E., Nuth, C., Gardelle, J., and Arnaud, Y.: Contrasting patterns of early 21st century
21 glacier mass change in the Himalaya, *Nature*, 488, 495–498, doi:10.1038/nature11324, 2012.
- 22 Krecl, P., Ström, J., and Johansson, C.: Carbon content of atmospheric aerosols in a residential area
23 during the wood combustion season in Sweden, *Atmos. Environ.*, 41, 6974–6985, 2007.
- 24 Lack, D. A. and Cappa, C. D.: Impact of brown and clear carbon on light absorption enhancement,
25 single scatter albedo and absorption wavelength dependence of black carbon, *Atmos. Chem. Phys.*, 10,
26 4207-4220, doi:10.5194/acp-10-4207-2010, 2010.
- 27 Lavanchy, V. M. H., Gäggler, H. W., Schotterer, U., Schwikowski, M., and Baltensperger, U.:
28 Historical record of carbonaceous particle concentrations from a European high-alpine glacier (Colle
29 Gnifetti, Switzerland), *J. Geophys. Res.*, 104, 21227–21236, doi:10.1029/1999JD900408, 1999.
- 30 Lim, S., Fäin, X., Zanatta, M., Cozic, J., Jaffrezo, J.-L., Ginot, P., and Laj, P.: Refractory black carbon
31 mass concentrations in snow and ice: method evaluation and inter-comparison with elemental carbon
32 measurement, *Atmos. Meas. Tech.*, 7, 3307-3324, doi:10.5194/amt-7-3307-2014.
- 33 Lutz, S., Anesio, A.M., Raiswell, R., Edwards, A., Newton, R.J., Gill, F., and Benning, L.G.: The
34 biogeography of red snow microbiomes and their role in melting arctic glaciers. *Nat. Commun.* 7:
35 11968, doi: 10.1038/ncomms11968, 2016.
- 36 Meinander, O., Kazadzis, S., Arola, A., Riihelä, A., Räisänen, P., Kivi, R., Kontu, A., Kouznetsov, R.,
37 Sofiev, M., Svensson, J., Suokanerva, H., Aaltonen, V., Manninen, T., Roujean, J.-L., and Hautecoeur,
38 O.: Spectral albedo of seasonal snow during intensive melt period at Sodankylä, beyond the Arctic
39 Circle, *Atmos. Chem. Phys.*, 13, 3793-3810, doi:10.5194/acp-13-3793-2013, 2013.
- 40 McConnell, J. R., Edwards, R., Kok, G. L., Flanner, M. G., Zender, C. S., Saltzman, E. S., Banta, J. R.,
41 Pasteris, D. R., Carter, M. M., and Kahl, J. D. W.: 20th century industrial black carbon emissions altered
42 arctic climate forcing, *Science*, 317, 1381–1384, doi:10.1126/science.1144856, 2007.
- 43 Ming, J., Cachier, H., Xiao, C., Qin, D., Kang, S., Hou, S., and Xu, J.: Black carbon record based on a
44 shallow Himalayan ice core and its climatic implications, *Atmos. Chem. Phys.*, 8, 1343– 1352,
45 doi:10.5194/acp-8-1343-2008, 2008.
- 46 Ming, J., Xiao, C., Du, Z., and Yang, X.: An Overview of Black Carbon Deposition in High Asia
47 Glaciers and its Impacts on Radiation Balance, *Adv. Water Resour.*, 55, 80–87, 2013.
- 48 Ming, J., Wang, Y., Du, Z., Zhang, T., Guo, W., Xiao, C., Xu, X., Ding, M., Zhang, D., and Yang,
49 W.: Widespread albedo decreasing and induced melting of Himalayan snow and ice in the early 21st
50 century. *PLoS One* 10(6):e0126235. doi:10.1371/journal.pone.0126235, 2015.
- 51 Painter, T. H., Barrett, A. P., Landry, C. C., Neff, J. C., Cassidy, M. P., Lawrence, C. R., McBride, K.
52 E., and Farmer, G. L.: Impact of disturbed desert soils on duration of mountain snow cover, *Geophys.*
53 *Res. Lett.*, 34, L12502, doi:10.1029/2007GL030284, 2007.

- 1 Painter, T. H., Skiles, S. M., Deems, J. S., Bryant, A. C., and Landry C.C.: Dust radiative forcing in
2 snow of the Upper Colorado River Basin: 1. A 6 year record of energy balance, radiation, and dust
3 concentrations. *Water Resources Research*, 48, doi: 10.1029/2012wr011985, 2012.
- 4 Qian, Y., Yasunari, T. J., Doherty, S. J., Flanner, M. G., Lau, W. K., Ming, J., Zhang, R.: Light-
5 absorbing particles in snow and ice: measurement and modeling of climatic and hydrological impact.
6 *Adv. Atmos. Sci.* 32(1), 64–91, doi: 10.1007/s00376-014-0010-0, 2015.
- 7 Qu, B., Ming, J., Kang, S.-C., Zhang, G.-S., Li, Y.-W., Li, C.-D., Zhao, S.-Y., Ji, Z.-M., and Cao, J.-J.:
8 The decreasing albedo of the Zhadang glacier on western Nyainqentanglha and the role of light-
9 absorbing impurities, *Atmos. Chem. Phys.*, 14, 11117–11128, doi:10.5194/acp-14-11117-2014, 2014.
- 10 Ruppel, M. M., Isaksson, E., Ström, J., Beaudon, E., Svensson, J., Pedersen, C. A., and Korhola, A.:
11 Increase in elemental carbon values between 1970 and 2004 observed in a 300-year ice core from
12 Høltedahlfonna (Svalbard), *Atmos. Chem. Phys.*, 14, 11447–11469, doi:10.5194/acp-14-11447-2014,
13 2014.
- 14 Raatikainen, T., Brus, D., Hooda, R. K., Hyvärinen, A.-P., Asmi, E., Sharma, V. P., Arola, A., and
15 Lihavainen, H.: Size-selected black carbon mass distributions and mixing state in polluted and clean
16 environments of northern India, *Atmos. Chem. Phys.*, 17, 371–383, doi:10.5194/acp-17-371-2017,
17 2017.
- 18 Schmitt, C. G., All, J. D., Schwarz, J. P., Arnott, W. P., Cole, R. J., Lapham, E., and Celestian, A.:
19 Measurements of light-absorbing particles on the glaciers in the Cordillera Blanca, Peru, *The*
20 *Cryosphere*, 9, 331–340, doi:10.5194/tc-9-331-2015, 2015.
- 21 Schwarz, J. P., Doherty, S. J., Li, F., Ruggiero, S. T., Tanner, C. E., Perring, A. E., Gao, R. S., and
22 Fahey, D. W.: Assessing Single Particle Soot Photometer and Integrating Sphere/Integrating Sandwich
23 Spectrophotometer measurement techniques for quantifying black carbon concentration in snow,
24 *Atmos. Meas. Tech.*, 5, 2581–2592, doi:10.5194/amt-5-2581-2012, 2012.
- 25 Schwarz, J. P., Gao, R. S., Perring, A. E., Spackman, J. R., and Fahey, D. W.: Black carbon aerosol size
26 in snow, *Nat. Sci. Reports*, 3, 1356, doi:10.1038/srep01356, 2013.
- 27 Shindell, D., Kuylensstierna, J. C. I., Vignati, E., van Dingenen, R., Amann, M., Klimont, Z., Anenberg,
28 S. C., Müller, N., JanssensMaenhout, G., Raes, F., Schwartz, J., Faluvegi, G., Pozzoli, L., Kupiainen,
29 K., Höglund-Isaksson, L., Emberson, L., Streets, D., Ramanathan, V., Hicks, K., Oanh, N. T. K., Milly,
30 G., Williams, M., Demkine, V., and Fowler, D.: Simultaneously Mitigating Near-Term Climate Change
31 and Improving Human Health and Food Security, *Science*, 335, 183–189, doi:
32 10.1126/science.1210026, 2012.
- 33 Svensson, J., Ström, J., Hansson, M., Lihavainen, H., and Kerminen, V.-M.: Observed metre scale
34 horizontal variability of elemental carbon in surface snow, *Environ. Res. Lett.*, 8, 034012,
35 doi:10.1088/1748-9326/8/3/034012, 2013.
- 36 Svensson J., Virkkula A., Meinander O., Kivekäs N., Hannula H.-R., Järvinen O., Peltoniemi J.I.,
37 Gritsevich M., Heikkilä A., Kontu A., Neitola K., Brus D., Dagsson-Waldhauserova P., Anttila K.,
38 Vehkamäki M., Hienola A., de Leeuw G. & Lihavainen H. 2016: Soot-doped natural snow and its
39 albedo — results from field experiments. *Boreal Env. Res.* 21: 481–503.
- 40 Thevenon, F., Anselmetti, F. S., Bernasconi, S. M., and Schwikowski, M.: Mineral dust and elemental
41 black carbon records from an Alpine ice core (Colle Gnifetti glacier) over the last millennium, *J.*
42 *Geophys. Res.*, 114, 102, doi: 10.1029/2008JD011490, 2009.
- 43 Virkkula, A., Ahlquist, N. C., Covert, D. S., Arnott, W. P., Sheridan, P. J., Quinn, P. K., and Coffman,
44 D. J. (2005). Modification, Calibration and a Field Test of an Instrument for Measuring Light
45 Absorption by Particles, *Aerosol Sci. Technol.* 39:68–83.
- 46 Warren, S. G., and Wiscombe, W. J.: A model for the spectral albedo of snow. II: Snow containing
47 atmospheric aerosols, *J. Atmos. Sci.*, 37, 2734–2745, 1980.
- 48 Wang, M., Xu, B., Zhao, H., Cao, J., Joswiak, D., Wu, G., and Lin, S.: The Influence of Dust on
49 Quantitative Measurements of Black Carbon in Ice and Snow when Using a Thermal Optical Method,
50 *Aerosol Sci. Technol.*, 46, 60–69, doi:10.1080/02786826.2011.605815, 2012.
- 51 Xu, B., Yao, T., Liu, X., and Wang, N.: Elemental and organic carbon measurements with a two-step
52 heating-gas chromatography system in snow samples from the Tibetan Plateau, *Ann. Glaciol.*, 43, 257–
53 262, 2006.

- 1 Xu, B., Cao, J., Hansen, J., Yao, T., Joswiak, D.R., Wang, N., Wu, G., Wang, M., Zhao, H., Yang, W.,
- 2 Liu, X., and He, J.: Black soot and the survival of Tibetan glaciers. *Proc. Nat. Acad. Sci. USA*, 106,
- 3 22114–22118, doi:10.1073/pnas.0910444106, 2009.
- 4 Yang, S., Xu, B., Cao, J., Zender, C. S., and Wang, M.: Climate effect of black carbon aerosol in a
- 5 Tibetan Plateau glacier, *Atmos. Environ.*, 111, 71–78, doi.org/10.1016/j.atmosenv.2015.03.016 1352-
- 6 2310, 2015.
- 7 Zhang, Y., Kang, S., Li, C., Gao, T., Cong, Z., Sprenger, M., Liu, Y., Li, X., Guo, J., Sillanpää, M.,
- 8 Wang, K., Chen, J., Li, Y., Sun, S.: Characteristics of black carbon in snow from Laohugou No. 12
- 9 glacier on the northern Tibetan Plateau, *Sci. Tot. Environ.*, 607-608, 1237-1249,
- 10 doi.org/10.1016/j.scitotenv.2017.07.100, 2017.

1 Table 1. Snow pit filter samples from Sunderdhunga 2015. Durga kot glacier snow pits are A-D and Bhanolti glacier snow pit E.

Snow pit ID and elevation (m a.s.l.)	Sample interval (cm)	τ_{TOT}	τ_D	τ_{EC}	EC TOM (g m ⁻²)	EC _{optical} (g m ⁻²)	eEC (g m ⁻²)	Total C (g m ⁻²)	EC ($\mu\text{g L}^{-1}$)	F _D
A, 4869	0-2	3.94	2.63	1.31	0.09	0.05	0.03	1.75	362.18	66.68
	2-5	-	-	-	0.25	0.00	-	0.25	1010.62	-
	5-10	-	-	-	0.30	0.01	-	11.11	1030.84	-
B, 4921	0-2	0.69	0.26	0.43	0.01	0.01	0.01	0.15	40.33	37.64
	2-6	-	4.79	-	0.13	0.04	-	4.24	398.60	-
C, 4921	0-3	0.29	0.16	0.13	0.01	0.00	0.00	0.21	35.71	56.62
	3-6	1.76	1.32	0.44	0.03	0.02	0.01	1.24	55.15	75.12
	6-9	-	5.19	-	0.15	0.00	-	4.88	1095.79	-
	9-13	2.20	1.35	0.84	0.06	0.03	0.02	0.76	381.63	61.57
D, 4950	0-5	0.11	0.07	0.04	0.00	0.00	0.00	0.06	13.20	66.65
	5-10	-	-	-	0.07	0.01	-	6.70	327.14	-
	10-20	1.37	0.94	0.43	0.04	0.02	0.01	0.64	220.21	68.63
	20-30	1.15	0.66	0.49	0.02	0.02	0.01	0.34	78.58	57.36
E, 5008	0-3	1.81	1.41	0.40	0.02	0.02	0.01	1.27	65.73	77.87
	3-6	3.25	1.97	1.27	0.08	0.04	0.03	1.45	272.57	60.77
	6-10	5.88	4.09	1.79	0.12	0.03	0.05	3.58	607.83	69.55
	10-15	2.94	1.77	1.17	0.06	0.04	0.03	0.97	233.21	60.32
	15-20	0.98	0.32	0.66	0.04	0.02	0.02	0.30	111.42	33.05
	20-30	1.06	0.52	0.54	0.02	0.02	0.01	0.23	140.71	49.15
	30-40	1.04	0.41	0.63	0.03	0.02	0.02	0.21	105.55	39.61
	40-50	1.03	0.38	0.65	0.02	0.02	0.02	0.21	98.15	36.71
	50-60	2.10	1.04	1.06	0.06	0.04	0.03	0.66	269.67	49.53
	60-70	2.75	1.10	1.65	0.07	0.06	0.04	0.49	179.30	39.90
70-80	1.21	0.44	0.77	0.02	0.02	0.02	0.19	93.00	36.12	
80-90	0.91	0.33	0.59	0.02	0.02	0.01	0.15	72.80	35.81	

90-100	1.65	0.73	0.92	0.04	0.03	0.02	0.31	143.80	43.95
100-110	0.57	0.17	0.40	0.02	0.01	0.01	0.15	79.31	29.54
110-120	0.46	0.12	0.34	0.02	0.01	0.01	0.15	56.91	25.68

1